CHEMICAL REVIEWS

Volume 109, Number 9

Thermochemistry of Microporous and Mesoporous Materials

Alexandra Navrotsky,* Olga Trofymluk,† and Andrey A. Levchenko‡

Peter A. Rock Thermochemistry Laboratory and NEAT ORU†, University of California at Davis, Davis, California 95616

Received October 23, 2008

Contents

1. Introduction 3885
2. Zeolites 3887
   2.1. General Remarks 3887
   2.2. Anhydrous High-Silica Zeolites 3889
   2.3. Anhydrous Aluminosilicate Zeolites 3891
   2.4. Zeolite Hydration and Cation Exchange 3891
3. Mesoporous Silica 3895
4. Interactions with Structure-Directing Agents 3895
5. Zeotypes 3896
6. Synthesis and Transformations of Zeolites and Related Materials 3897
7. Concluding Remarks 3899
8. References 3900

1. Introduction

The past two decades have seen exciting advances in the discovery, improved synthesis, processing, and molecular-level engineering of new inorganic materials having specialized electronic, ceramic, and structural applications. Many such materials share two common characteristics: they are complex in structure and composition and they must be prepared by a series of steps under carefully controlled conditions. The use of low-temperature aqueous synthesis conditions, with appropriate attention to pH, inorganic and organic structure-directing agents, and subsequent drying and calcination protocols has led to a wealth of new and often metastable crystalline polymorphs, to amorphous materials, and to fine powders with particles of nanoscale dimensions. Such materials are not constrained to be in chemical equilibrium with their surroundings and do not necessarily represent the state of lowest free energy. The abundance of possible new structures formed begins to mimic the riches of organic chemistry, where the fact that all complex organic and biological molecules are metastable under ambient conditions with respect to a mixture of carbon dioxide, water, and other simple gases is irrelevant except in a conflagration.

Liberation of ceramic science from the tyranny of high-temperature equilibrium thus is leading to *new materials synthesized more quickly, at lower cost, and under environmentally more friendly conditions.* There is, of course, a price to pay. First, the synthetic procedures are more complex than traditional "mix, grind, fire, and repeat" ceramic processing. Second, and more importantly, *relatively little is known about the long-term stability in either a thermodynamic or a kinetic sense, of the materials formed, about their degradation during use, and about materials compatibility*. Two examples of such problems are the potential corrosion of materials by ambient H_2O and CO_2 and the collapse to inactive phases of complex zeolitic and mesoporous catalysts under operating conditions. Chemical reactions in metastable materials are governed by an intertwined combination of thermodynamic driving forces and kinetic barriers. For this rich landscape of new materials, neither the depths of the valleys nor the heights of the mountains are known; indeed, one cannot even always tell which way is energetically downhill.

Families of microporous and mesoporous (synthetic and natural) framework materials promise applications for a better and greener future. Aluminosilicate zeolites are by far the most familiar members of a larger group of crystalline porous materials with pore sizes less than 2 nm. They have found many uses in industrial and domestic settings including applications in the petrochemical industry as catalysts for petroleum cracking, agriculture as soil treatments, medicine for production of medical-grade oxygen, nuclear waste disposal, water purification, and detergents. Despite tremendous efforts undertaken by many groups around the world, a complete understanding of underpinning fundamental principles that govern formation of zeolites and mesoporous materials is still missing. This presents limitations to the discovery of new frameworks with optimized properties.

What, then, is the role of the thermodynamics and thermochemical measurements for these new and exciting materials? Enthalpies and free energies of formation and the energetics of metastability are useful in two major contexts. The first is thermochemical data for the calculation of phase relations, of materials compatibility, and of optimal synthesis

* To whom correspondence should be addressed: anavrotsky@ucdavis.edu.
† Nanomaterials in the Environment, Agriculture and Technology - Organized Research Unit
‡ Current address: Setaram Inc, Newark, California 94560

10.1021/cr800495t CCC: $71.50
Published on Web 07/28/2009

Alexandra Navrotsky holds the Edward Roessler Chair in Mathematical and Physical Sciences and is a Distinguished Professor of Ceramic, Earth, and Environmental Materials Chemistry at the University of California, Davis, where she is the director of the Organized Research Unit on Nanomaterials in the Environment, Agriculture and Technology (NEAT-ORU) and the Peter A. Rock Thermochemistry Laboratory. Her research relates microscopic features of structure and bonding to macroscopic thermodynamic behavior in minerals, ceramics, and other complex materials. She has published over 500 scientific papers. Recent awards include the Benjamin Franklin Medal in Earth Science (2002), the Urey Medal of the European Association of Geochemistry in (2005), the Spriggs Phase Equilibria Award of the American Ceramic Society (2005), the Rossini Lectureship Award at the 19th International Conference on Chemical Thermodynamics (2006), the Harry H. Hess Medal of the American Geophysical Union (2006), and the Roebling medal of the Mineralogical Society of America (2009). She was elected to the National Academy of Sciences in 1993, and in 1995 she was awarded the degree of Doctor Honoris Causa from Uppsala University, Sweden. She serves on numerous advisory committees and panels in both government and academe.

Andrey A. Levchenko joined the Peter A. Rock Thermochemistry Laboratory (University of California—Davis) as a postdoctoral researcher after completing his Ph.D. in condensed matter physics at the Russian Academy of Sciences in 2002. He has been a recipient of scholarships for excellence in graduate research from Russian Academy of Sciences and Ministry of Education, as well as Russian President Fellowship for studying abroad (2000). His research interests include energetics and structure−property relationships in organic−inorganic materials, inorganic materials, and nanoparticles. He utilizes thermal analysis and calorimetry, as well as complementary experimental tools including diffraction methods, spectroscopic and microscopic techniques, and neutron scattering, to study driving forces of self-assembly, confinement and related phenomena at solid−solid and solid−liquid interfaces such as water on oxide nanoparticles and organic glass-forming liquids in solid matrices. He currently leads the Setaram-U.S. Laboratory for Advanced Calorimetry and Gas High-Pressure Analysis in Newark, California. (Setaram Inc. is a U.S. subsidiary of Setaram Instrumentation, Caluire, France, a leading manufacturer of advanced systems for thermal analysis, high-pressure gas sorption, and calorimetry.)

Olga Trofymluk is a staff research associate in the Peter A. Rock Thermochemistry Laboratory and NEAT ORU. After completion of the M.S. thesis at Lviv Polytechnic University (Lviv, Ukraine) with *summa cum laude* in biotechnology, she did her Ph.D. on thin polymer films working with Prof. Voronov (Lviv Polytechnic University, Ukraine) and Prof. Stamm at Max-Plank Institute for Polymer Research (Mainz, Germany). She joined Peter A. Rock Thermochemistry Laboratory (University of California—Davis) as a postdoctoral researcher after finishing her Ph.D. with highest honors and working shortly at the Russian Academy of Sciences. She uses synthetic and calorimetric methods to study the energetics of inorganic porous and zeolite-like materials. She also applies numerous calorimetric and spectroscopic techniques to elucidate dynamics and energetics of confinement of organic molecules and water in porous matter.

conditions. Such equilibrium calculations are viewed by some as mundane. They are indeed mundane in the sense of being pertinent to the real world and essential for rational design of processing, fabrication, and encapsulation of components for lowest cost and longest life. Here the abundance of new materials has simply outrun the thermochemical database. The second area of relevance of energetics is in providing insight into the factors relating to structure, bonding, stability, and reaction mechanisms. Are many different structures accessible, what is their energetic cost, and what microscopic features (for example, cation size, bond angles, bond lengths, covalency) favor or limit the formation of a given structure? Such systematic understanding puts synthesis into a more rational and predictable context. The wealth of structures and complexity of interactions suggest an energy landscape, with small differences in energetics defining many local minima in free energy.

This review focuses on the energetics of two particular classes of generally metastable materials, the mesoporous and microporous framework structures, represented by zeolites and their relatives. There are a number of excellent reviews dedicated to synthesis and structure of zeolite and mesoporous materials. Some touch upon the subject of thermochemistry of these materials, but none of them provide a comprehensive and rigorous summary of thermodynamic properties in a systematic fashion. Cundy and Cox gave the most complete account of "the discoveries and advances in thinking in the field of zeolite synthesis from the 1940s up to late 2002" in the 2003 review[1] and revisited the topic in their 2005 review.[2] They also provided an exhaustive list of previous reviews on subjects related to zeolites synthesis and structure.[1] An important review focusing on structure and topology of zeolites and related materials has been published by Smith.[3] The nomenclature and structure of zeolites are given in a number of publications by the *International Zeolite Association* (IZA) Structure Commission.[4,5] In an earlier 1997

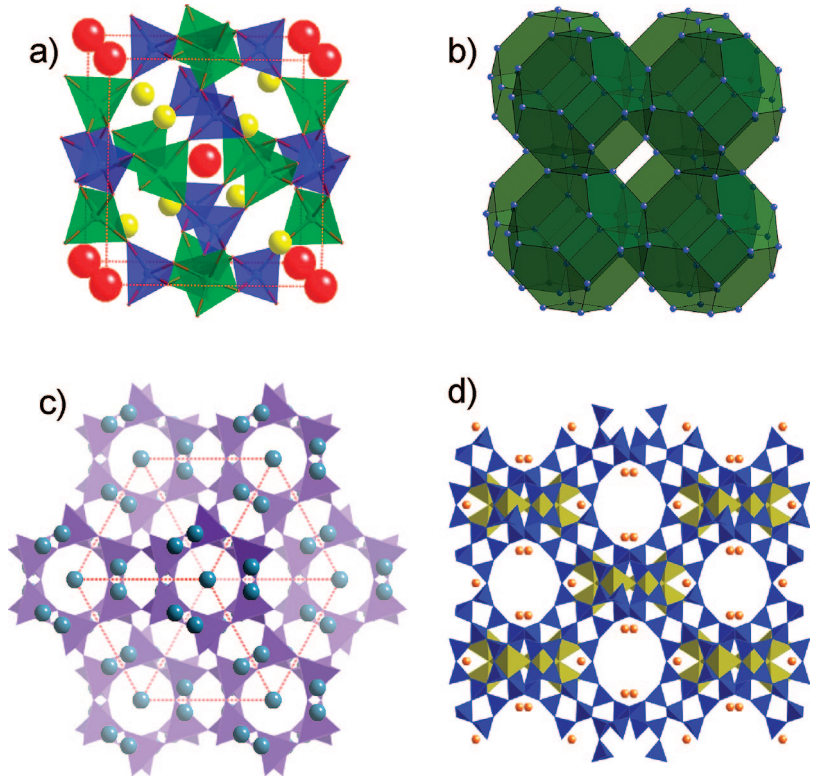

Figure 1. (a) Sodalite structure, $Na_8[AlSiO_4]_6Cl_2$. Note β-cages that contain alternating SiO_4 (green) and AlO_4 (blue) tetrahedra, and a central anion (yellow) surrounded by tetrahedrally coordinated cations (red). (b) Sodalite β-cage structure is composed of cubo-octohedra (green) with Si and Al atoms at the apexes. (c) Chabazite (CHA) structure, $CaAl_2Si_4O_{12}\cdot 6H_2O$. Ca atoms are light blue. Al and Si tetrahedra are purple. (d) Faujasite (FAU) structure, $(Na_2,Ca,Mg)_{3.5}Al_7Si_{17}O_{48}\cdot 32H_2O$. Na, Ca, and Mg octahedra are yellow. Al and Si tetrahedra are blue. Water molecules are orange.

review on zeolitic materials, Corma[6] outlined their synthesis and uses for catalytic applications. Accounts of catalytic applications of mesoporous materials are also given by Taguchi and Schuth.[7] Corma and Davis[8,9] analyzed advances in fabrication of new porous solids with ordered structures tailored to a variety of applications and highlighted future directions in the synthesis of low-density zeolites and related materials. The review by Ŝefĉík and McCormick, published a decade ago,[10] gave a detailed outline of the aqueous equilibria of silicate solutions and laid the foundation for further studies of solution thermodynamics and crystallization diagrams of zeolite.[11−13] Rimer et al.[14] summarized recent developments in analyses of self-assembly and growth of zeolite nanoparticles from the viewpoint of structure and solution equilibria. Progress in computer simulations of zeolite growth using molecular templates is reported in a recent review by Sastre.[15] Synthesis of aluminophosphates is discussed by Yu and Xu.[16]

2. Zeolites

2.1. General Remarks

Zeolites comprise a wide range of structures and composition. Up to date (Jul 2009), the International Zeolite Association (IZA) Structure Commission has assigned 179 Framework type Codes corresponding to distinctive zeolite topologies with a few new structures being added each year.[4]

The TO_4 tetrahedron is the basic building block in zeolites with T usually being silicon with common substitution by aluminum. Naturally occurring zeolite minerals are typically hydrated aluminosilicates.[17,18] They contain alkali and alkaline cations and water molecules in large channels or cavities within a porous framework formed by joining AlO_4 and SiO_4 tetrahedra at their apexes, with each tetrahedron being linked to four others (see Figure 1). Synthetic zeolites including silica-rich modifications and anhydrous pure SiO_2 materials with a large number of zeolite frameworks (some analogous to natural zeolites, many new) have been the focus of intense synthetic effort. Thus, the aluminosilicate zeolites can be structurally related to the pure silica materials by the following substitution scheme.

$$Si^{4+}\ (\text{in framework}) = Al^{3+}\ (\text{in framework}) + 1/n\ M^{n+}\ (\text{in channel or pore}) \quad (1)$$

The IUPAC has developed recommendations for how to write a crystal chemical formula of a zeolite per crystallographic unit cell as shown in the following scheme.[19]

$$|\text{guest composition}|[\text{host composition}]_h \{\text{host structure}\}_p\{\text{pore structure}\}(\text{Sym}) \quad (2)$$

However, other methods are used in the literature. For example, chabazite (CHA, Figure 1c), a common mineral and synthetic material, can be idealized in its pure calcium and fully hydrated form, to be $CaAl_2Si_4O_{12}\cdot 6H_2O$, reflecting a formula with the smallest integral number of atoms. However, a unit cell of this material is based on 24 oxygens, and the formula is often given as $Ca_2Al_4Si_8O_{24}\cdot 12H_2O$. When energetics of the framework are compared with the parent compound, silica, SiO_2, from which all framework structures can be derived, we choose to use a two-oxygen formula unit (or mole of tetrahedra TO_2, T= metal in tetrahedra), which gives chabazite the formula $Ca_{1/6}Al_{1/3}Si_{2/3}O_2\cdot H_2O$, with the

anhydrous form falling 1/3 of the way across the $xCa_{0.5}AlO_2-(1-x)SiO_2$ join.

The hydration of a zeolite can be presented in a general form as

$$(M^{n+})_{x/n}Al_xSi_{1-x}O_2 + mH_2O = (M^{n+})_{x/n}Al_xSi_{1-x}O_2 \cdot nH_2O \quad (3)$$

Substitution of silicon with phosphorus, germanium, or other metals creates another emerging class of zeolite-like materials or zeotypes that are also considered in this review. The aluminophosphate (such as $AlPO_4$) and gallophosphate (such as $GaPO_4$) are families of substitution of tetravalent silicon by a trivalent and a pentavalent cation, with no extraframework cations

$$2Si^{4+} = Al^{3+}(\text{or } Ga^{3+}) + P^{5+} \quad (4)$$

In aluminosilicate zeolites, the degree of Al−Si order in the framework can be variable (and is often unknown), whereas in aluminophosphates, the Al^{3+} and P^{5+} ions alternate in a fully ordered array. This alternation of charges in such III−V frameworks results from relative instabilities of Al−O−Al and P−O−P linkages, and leads to only structures containing rings with even numbers of tetrahedra.[16] The number of aluminophosphate open frameworks can be significantly extended by including interrupted ionic frameworks with the Al/P ratio less than one.[16] These ionic frameworks add to the riches of open framework materials that find almost no analogues among zeolites. The rear examples of zeolite interrupted frameworks include partheite (-PAR), SSZ-74 (-SVR), and a few others. They decompose upon template removal. No thermochemical data are available for them, and they are not discussed further in this review.

The accessible internal surfaces and pore volumes within the channels form a unique environment for controlled chemical reactions. Synthetic zeolites represent a multimillion dollar industry, with applications ranging from catalytic cracking of petroleum, to gas separations, to detergents.[6,18,20] Creation of new zeolite frameworks and compositions, with cage size and acidity tailored to specific applications, continues to be an active area of both academic and industrial research.[1,21−23] Yet, until recently, it was generally assumed that most zeolites are metastable phases whose synthesis is controlled by kinetics and aided by molecules added as "templates" or "structure-directing agents". The extent of metastability, the differences in energy between different framework topologies for the same composition, and the effect of compositional variation on energetics could only be subjects of speculation.[24] Recent thermochemical data, obtained largely by high-temperature oxide melt solution calorimetry, have begun to fill in the details of zeolite energetics.[25−29]

Thermodynamic stability should not be confused with "thermal stability" in terms of kinetics. Thermal stability from a kinetic point of view is related to experimental conditions under which a metastable material decomposes on heating. As shown in this review, zeolites are synthesized under conditions where they are thermodynamically stable with respect to the starting materials (aqueous solutions, gels, nanoparticles); thus, their formation reactants are, and indeed must be, "downhill" in free energy. In contrast, their anhydrous forms are greatly metastable with respect to anhydrous assemblages of denser phases.

From the viewpoint of practical applications, it is highly desirable to construct thermally and hydrothermally stable materials with large pores.[30,31] Although zeolites are well-studied microporous materials with highly organized crystalline structure, their channel dimensions are limited to less than 1 nm.[9] A major challenge for synthetic chemists is to overcome this limitation and design ordered frameworks with large pores. Larger pores from 2 to 50 nm are now easy to obtain in mesoporous silica molecular sieves with amorphous walls.[32,33] Emerging and promising applications of these materials now include not only catalysis, separation, and ion exchange[6,7,9,34,35] but also more unusual uses such as contrast agents for diagnostic magnetic resonance imaging,[9,36] hosts for laser dyes[37] and templates for metal nanowires,[38−40] semiconductor nanowires,[41,42] carbon nanotubes, and polymer−carbon composites.[43]

This review focuses on several related questions. (1) What is the effect of framework type on the enthalpy, entropy, and free energy of a zeolite of a given composition? (2) For a given framework, what are the energetics of ionic substitutions (e.g., as in eqs 1 and 4), and how does the enthalpy of a given substitution vary with the framework type? When the substitution involves different cations (e.g., Na and K), the thermochemical data are directly relevant to ion exchange. (3) What are the thermodynamics of hydration and how do they vary with framework type and composition? (4) As controlled by the systematics above, which zeolites have thermodynamic stability fields and which are purely metastable phases? (5) What do the systematics above imply for zeolite synthesis and the role of the structure-directing agent (SDA)? What other energetic information is available about framework−SDA interactions? These issues are relevant to a number of other phenomena that will not be touched upon in this review. The energetics of hydration and cation binding clearly help define the "acidity" of a given framework site and its ability to bind other molecules and catalyze reactions. The relations between thermodynamics and kinetics, between driving forces and rates of reaction, will not be reviewed here. Reflecting the thermodynamic emphasis of this review, little discussion will be offered regarding the mechanisms of zeolite formation and reactions in the pores, though energetics play a crucial role in defining possible pathways.

In this context, computer-assisted thermodynamic calculations offer additional insights into energetics of framework structures. Quantum mechanical (QM) calculations and molecular dynamic (MD) studies of zeolites are computationally demanding because the zeolite crystallographic unit cells may contain hundreds of atoms. Therefore, many simulations, especially ab initio calculations, are performed on smaller, cluster systems. In MD simulations, force-field potentials are parametrized to accurately describe interatomic interactions and resulting structures. The accuracy of energy calculations is a sticking point even for the most comprehensive QM methods. The 1 kcal/mol (4 kJ/mol) accuracy milestone for predicting lattice energies is still to be overcome by QM and MD methods, while calorimetry obtains errors of about ±1 kJ/mol (per mole of tetrahedra). The accuracy of predicted formation enthalpies is often no better than 10 kJ/mol.[44]

The extensive body of studies on zeolites employing computational methods can be divided into two main groups

that concern (1) stability/formation energetics of zeolitic structures including location and ordering of cations within the framework and their interaction with the framework and (2) interactions of the zeolite framework with atoms and molecules that are not part of the zeolite structure.

The first group of studies deals with calculations of equilibrium geometry/structure and relative stabilities of zeolites. The essence of these studies lies in identifying the most stable configurations and finding structures with the lowest formation energy by energy minimization methods.[45,46] In this regard, computational studies by density functional theory (DFT) and molecular mechanics (MM) have been very useful in structure refinement studies of zeolites in which structure determination cannot be done by experimental X-ray and neutron diffraction methods alone.[45,47,48] The second large group of studies covers a wide range of topics including investigations into adsorption of guest atoms and molecules, host−guest chemistry, and acid−base and catalytic properties of zeolites.[49] Much progress has been made in identifying preferential sites of adsorption, catalytic activity and pathways of catalytic reactions, and calculating adsorption energies and diffusion coefficients of guest molecules.[50−53] Calculations by DFT and MD methods and identification of vibrational modes in IR spectra and chemical shifts in NMR data of guest molecules are important in assessing catalytic activity.[50,54,55] Water plays an important role in this class of host−guest systems. Ab initio methods have been widely used to calculate hydration of aluminosilicate and aluminophosphate zeolites, e.g., location and distribution of framework water.[56−61]

Along the same lines, experimental data on energetics, primarily obtained by calorimetry, are essential to deriving refined forcefields for MD and MM calculations of zeolites containing extraframework cations, water, and other guest molecules such as aromatics.[24,57,62−66] This review is not aimed at giving either a representative overview of computational methods or in-depth analysis of results obtained by these methods. Readers are referred to various reviews and journal articles on the subject.[1,15,44,53] Yet a few important computational works on the subject of the review will be discussed.

2.2. Anhydrous High-Silica Zeolites

The energetics of silica-based materials including silica gels, glasses, and microporous and mesoporous materials have been studied extensively by high-temperature oxide melt solution calorimetry over the past ten years (see Table 1 and Figure 2). In particular, Petrovic et al.[67] found that the range of energies in anhydrous silica zeolites is quite narrow (6.8−14.4 kJ/mol above quartz). The study by Piccione et al.[27] extended the earlier work[67] of Petrovic et al.[67] to a larger range of better-characterized materials and drew similar conclusions (see Figure 2).

Since amorphous silicas derived from gels are higher in energy than fused glass by 0−10 kJ/mol, silica zeolites and amorphous silicas occupy an overlapping range of energies.

For a discussion of zeolite synthesis and overall picture of the framework energetics, it is important to compare the metastability of anhydrous silica to that of species in the "mother liquor". In a hydrothermal synthesis, components in the mother liquor, which include a silica source, a base, and an SDA, undergo a series of continuous and sometimes stepwise transformations to form the final framework. These transformations are governed by energetics of interactions between the components, reflecting both thermodynamic driving forces and kinetic barriers. Thermodynamic parameters provide a means to calculate the thermodynamic driving forces that influence terms in kinetic equations governing the rates of decomposition, crystallization, dissolution, phase separation, and other processes. The product of the gas constant and the absolute temperature, RT, is a suitable reference to compare the average available thermal energy to the energetic "cost" of metastable products or intermediates. At 373 K, a typical synthesis temperature, this available thermal energy is only 3.1 kJ/mol. Therefore, energetic barriers of this magnitude can be overcome through a series of transformations involving interactions among the components in the "mother liquor". Since the energy (and free energy) differences between amorphous silica and various frameworks is often of the same magnitude, this suggests that formation of a zeolite framework from amorphous silica is not hindered energetically under typical synthesis conditions.

Figure 2 shows a consistent trend among zeolitic silicas, mesoporous silicas, and aluminophospate. Their enthalpy relative to quartz increases with increasing molecular volume (MV) but seems to level off at values near 30 kJ/mol. There have been attempts to reveal a more detailed picture of the stability landscape for silica zeolites by finding correlations between microstructure of the framework (presence of strained rings) and framework stability. Yet calorimetric experiments suggest complex interactions among different factors affecting overall energy landscape of a given framework. The formation enthalpy data for MEI (ZSM-18), a silica zeolite with three-membered rings, exemplify these effects. The enthalpy for MEI (13.9 kJ/mol above quartz) lies some 3 kJ/mol higher than that of EMT having similar molar volume but no three-membered rings (see Figure 2). Similarly, the enthalpy of moganite, a structure derived from quartz by twinning on the unit cell scale, with a volume similar to quartz but probably containing strained rings at the twin boundaries, lies some 3 kJ/mol above that of quartz. In contrast, FAU has enthalpy and molar volume values similar to those of MEI but has no three-membered rings. These observations, plus the fact that coesite, a high-pressure SiO_2 polymorph denser than quartz, is higher than quartz in enthalpy at atmospheric pressure, definitely show that energy does not scale in any simple monotonic fashion with MV (or framework density (FD)) if energy resolution better than the thermal energy is required. On a large energy scale (resolution $\approx 2RT$), formation enthalpies of high-silica zeolites and mesoporous silicas increase nonlinearly with MV (see Figure 2), imposing little energetic limitations to the synthesis of these structures.

Boerio-Goates et al.[68] showed by heat capacity measurements using adiabatic calorimetry that the entropic factors ($T\Delta S$ term) for several silica zeolite frameworks are not dominant in zeolite stability. Different silica frameworks have almost identical standard entropies (S^0_{298}), reflecting the strong tetrahedral bonding in the framework. Yet the entropic contribution could be important when considering the high-temperature behavior of zeolites. Some theoretical studies[73,74] predict high-temperature stability fields for zeolites such as MFI stemming from the increasing role of entropy in the overall free energy of formation, but this has not been seen experimentally.

Computational studies have been important in understanding correlations that might exist between framework instabilities and specific structural parameters. Early studies of

Table 1. Thermodynamic and Structural Properties of Selected Microporous and Mesoporous Materials

framework	framework density, Si/nm^3	molar volume, cm^3/mol	ΔH_{trans}^{298}, kJ/mol of TO_2	ΔS_{trans}^{298} [a], J/(K·mol)	ref
AFI	17.80	33.83	7.2		27
AST	17.29	34.83	10.9 ± 1.18		27
BEA	15.60	38.60	9.3 ± 0.82	44.9 ± 0.1	27, 28, 68
CFI	18.28	32.94	8.8 ± 0.81		27
CHA	15.40	39.10	11.4 ± 1.47		27
EMT	13.0	46.51	10.5 ± 0.9		67
FAU	13.45	44.77	13.6	44.7 ± 0.1	27, 28, 68
FER	18.43	32.67	6.6		27
IFR	17.03	35.36	10.0 ± 1.17		27
ISV	15.36	39.21	14.4 ± 1.07		27
ITE	16.26	37.04	10.1 ± 1.21		27
MEI	14.2	42.12	13.9 ± 0.4		67
MEL	17.80	33.83	8.2 ± 1.34		27
MFI/F	17.97	33.51	6.8 ± 0.80	45.1 ± 0.1	27, 28, 68
MFI/OH	17.97	33.51	8.01 ± 0.82	46.3 ± 0.2	27, 28, 68
MTW	19.39	31.06	8.7		27
MWW	16.51	36.47	10.4 ± 1.45		27
STT	16.83	35.78	9.2 ± 1.22		27
quartz	26.52	22.71	0.0	41.5 ± 0.1	27, 28, 68
cristobalite	23.37	25.77	2.84	43.4 ± 0.1	27, 28, 68
moganite	26.22	22.97	3.4		27
coesite	29.26	20.58	2.93	38.5 ± 0.3	27, 28, 68
tridymite	22.61	26.63	3.21	43.9 ± 0.4	27, 28, 68
0.33Ge-ITQ-21	14.03	42.91	21.88 ± 0.35		69
0.09Ge-ITQ-21	14.29	42.12	20.89 ± 0.22		69
0.05Ge-ITQ-21	14.47	41.60	18.94 ± 0.41		69
0.24Ge-ITQ-22	17.53	34.34	14.82 ± 0.47		69
0.20Ge-ITQ-22	17.57	34.26	14.79 ± 0.33		69
0.11Ge-ITQ-22	17.68	34.05	14.71 ± 0.42		69
$CaSi_2O_5$			7.60 ± 4.27		70
berlinite		23.23	0 ± 0.54		71
$Al_{0.5}P_{0.5}O_2$-5		34.27	7.0 ± 2.15		71
$Al_{0.5}P_{0.5}O_2$-8		34.32	5.56 ± 1.42		71
$Al_{0.5}P_{0.5}O_2$-11		30.44	6.18 ± 1.17		71
$Al_{0.5}P_{0.5}O_2$-42		42.01	7.82 ± 1.94		71
VPI-5		42.26	8.38 ± 2.26		71
MCM-41_3		71.59	19.33 ± 0.98		72
MCM-41_4		72.79	18.96 ± 0.49		72
SBA-15_5		110.04	23.20 ± 0.56		72
SBA-15_6		102.83	23.49 ± 0.39		72
SBA-15_7		66.78	24.72 ± 0.54		72
SBA-15_8		100.43	24.54 ± 1.38		72
SBA-15_9		93.82	26.11 ± 0.99		72
SBA-15_10		104.63	25.76 ± 1.53		72
SBA-15_11		96.22	25.22 ± 1.29		72
SBA-15_12		131.07	24.58 ± 0.81		72
SBA-15_15		107.64	27.12 ± 0.88		72
SBA-15_19		86.61	26.70 ± 0.48		72
SBA-15_22		87.81	27.59 ± 0.50		72
SBA-15_24		145.49	31.39 ± 0.94		72
SBA-15_26		167.12	31.32 ± 1.53		72
MCM-48_2		72.19	24.68 ± 0.74		72
MCM-48_3		75.79	25.06 ± 0.61		72
SBA-16_4		58.97	26.60 ± 0.37		72
SBA-16_5		61.97	24.62 ± 1.13		72

[a] Measurements of heat capacities necessary to calculate entropies are labor-intensive and have traditionally required large samples. Thus, the number of zeolites for which such measurements have been made is limited.

energetics of silica zeolites[74,75] were purely theoretical, as no reliable thermochemical data were available at the time. Kramer et al.,[76] Civalleri et al.,[77] and de vos Burchart et al.[78] established the basis for further studies by presenting calculated formation enthalpies for a wide array of zeolites. They noted that energetics of zeolites are similar within 10 kJ/mol, and there is a linear correlation between the energetics of zeolite and FD. These calculations were done using empirical forcefields. The work by Petrovic et al.[67] spurred a new wave of research into energetics of zeolites using modern computational methods.[55,73,79−89] Ab initio calculations on both molecules and extended systems have suggested that Si−O−Si bond angles below 135° destabilize zeolitic structures.[90]

There has been extensive computational work attempting to predict energetic stability, pore-volume relationships, and flexibility of existing and hypothetical zeolite frameworks, mostly in their siliceous forms. The main objectives have been to assess the plausibility of their successful synthesis and application in novel processes. Examples include studies by Foster et al.,[80−82] Zwijnenburg et al.,[85,86,88] and others[91,92] that compare enthalpies of formation for a range of SiO_2 phases, namely, siliceous zeolites and SiO_2 dense polymorphs. The energetics calculated using DFT show an overall

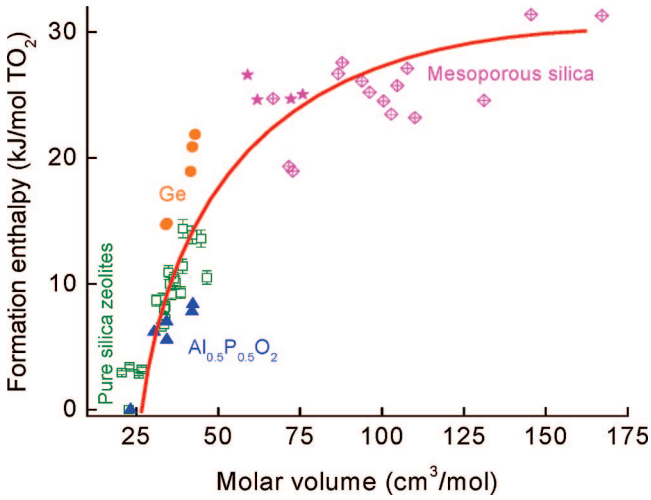

Figure 2. Formation enthalpies for silica zeolites, Ge and Al phosphate zeotypes, and mesoporous silica: green symbols, dense and zeolitic silica phases; blue symbols, aluminophosphates; orange symbols, Ge-zeolites; magenta symbols, mesoporous silica cubic (stars) and hexagonal (diamonds).

linear correlation with measured values, but both considerably underestimated or overestimated computed enthalpies are often observed.[88]

Utilizing methods of molecular mechanics, Moloy et al.[93] calculated internal surface areas for a number of zeolite structures and showed that the energetics can be correlated with internal surface area, giving a surface energy of 0.09 J/m^2, comparable to that of amorphous silica.[94] This rather small surface energy and the dominance of internal over external surface area explains why the enthalpy of silica MFI does not depend on particle size (in the particle size range >40 nm) as demonstrated by solution calorimetry of Li et al.[95]

2.3. Anhydrous Aluminosilicate Zeolites

Navrotsky and Tian[96] systematically analyzed how energetics of anhydrous aluminosilicate zeolites depend on framework type, aluminum content x = Al/(Al + Si), and charge-balancing cation (eq 1), and compared their energertics with those of corresponding aluminosilicate glasses. This work was a continuation of an earlier study by Petrovic and Navrotsky[26] on Na−FAU with varying Si/Al ratios. The calculated formation enthalpies for a series of the glasses with M = Li, Na, K, Rb, Cs, Mg, Ca, Sr, Ba, and Pb, reported by Roy and Navrotsky,[97] have been shown to fan out with increasing endothermic slopes as the basicity of the charge-balancing cation increases (Figure 3a).

The calorimetric data[96] for zeolites with different cations (Li, Na, K, Rb, Cs, Mg, Ca, Sr, Ba, and Pb) suggest energetic trends similar to those seen in glasses (Figure 3b). Table 2 lists, on a two oxygen basis, the enthalpies of several anhydrous alkali and alkaline earth aluminosilicate zeolites, reflecting different degrees of framework openness, compared to the dense stable phase assemblages and the glass. Figure 4 shows measured enthalpies of formation for several sodium aluminosilicate systems: glasses, dense stable phases (quartz, enpheline, feldspar), and a series of zeolites. The vertical displacement of the approximately parallel lines observed reflects the small enthalpies associated with the differences in structure, dense framework versus zeolite versus amorphous, as discussed above. The paralleled trends strongly suggest that the enthalpy of the substitution reaction (eq 1) is approximately constant for a given cation, independent of the details of long-range structure. These general trends apply to other charge-balancing cations in a variety of other structures,[96] implying that they can be used to predict energetics of framework structures in general.

Enthalpies of substitution for glasses, dense phases, and zeolites as a function of the ionic potential suggest a trend of increasing stabilization (more negative slope) with decreasing ionic potential (Figure 5).

Therefore, in anhydrous aluminosilicate zeolites, the energetics of substitution of Al and a charge-balancing alkali or alkaline earth cation follow similar trends as in corresponding glasses. The most stable substitutions are those involving large alkalis. These correlations form a useful predictive tool for zeolite energetics and ion exchange (at least in systems that are anhydrous or only weakly hydrated).

2.4. Zeolite Hydration and Cation Exchange

Negatively charged zeolite and zeolite-like frameworks can accommodate a wide variety of extraframework cations, including Na^+, K^+, Ca^{2+}, Mg^{2+}, and many others. These cations are relatively loosely held and can readily be exchanged for others in an aqueous solution. This property of zeolites is exploited in ion exchange in water purification, softening, and other uses. The broad field of ion exchange is not the focus of this review, and the reader is directed to several comprehensive reviews.[98,99]

The extensive internal volume of zeolitic frameworks may not be fully occupied by charge-compensating cations, leaving room for molecules such as water to enter the cages. Water can hydrate cage-residing cations, go into various adsorption sites offered by the framework geometries, or form clusters of various sizes. Water in high-silica zeolites shows distinct behavior because these frameworks are much less hydrophilic than those of aluminosilicates and they contain no charge-balancing cations.[17] Considerable interest has been drawn recently to pressure-induced hydration of hydrophobic zeolites because there are many interesting phenomena and water structures occurring at high water pressure far from equilibrium conditions of typical zeoilite synthesis.[100−102]

These multiple mechanisms of water incorporation complicate the picture of cation/water molecule packing and free energy landscape. In this section we first make some general observations and then present examples of the complex behavior for a number of specific systems.

The first general observation is that the incorporation of water is most exothermic at low water content and becomes less exothermic with increasing hydration.[103] In some zeolites, hydration occurs stepwise, with distinct phases of stoichimetric water content.[104,105] In other zeolites, water molecules show a *continuum* of energetics seen as a gradual and continuous change in water content and in the partial molar hydration enthalpy and no distinct change in structure.[57,103]

A second general feature is that hydration stabilizes the zeolite, often enough to give the hydrated open framework phase a true thermodynamic stability field near room temperature, with the favorable hydration energy (20−40 kJ/mol of water relative to liquid H_2O) compensating the metastability (7−15 kJ/mol of TO_2) of the anhydrous framework with respect to dense structures such as quartz, feldspar, or nepheline. The energetically favorable but entropically costly interactions leading to the observed enthalpy−entropy correlation are those of water molecules

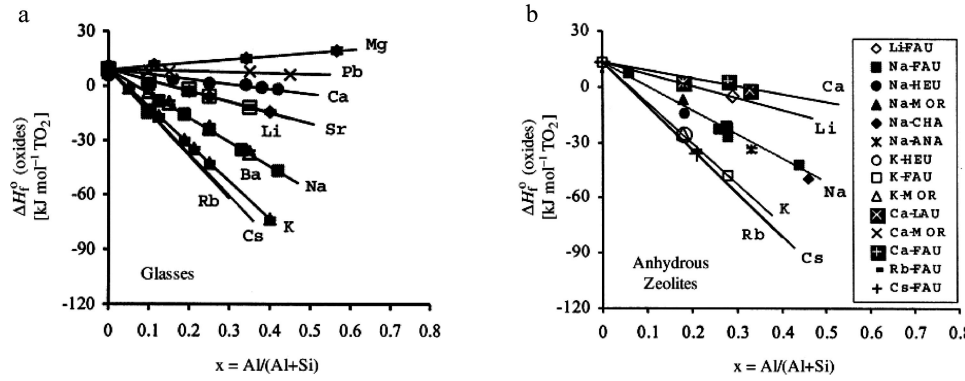

Figure 3. Comparison of the enthalpies of formation at 298 K from the oxides as a function of x = Al/(Al + Si) for dense phases, glasses, and zeolites of Na^+. Reprinted with permission from ref 96. Copyright 2001 John Wiley & Sons, Inc.

Table 2. Measured Enthalpies of Formation of Anhydrous Zeolites at 298 K, Per Mol of Tetrahedra

x[a]	structure[b]	formula	$\Delta H^0_{f(oxides)}$, kJ mol^{-1} of TO_2	ref
0.292	Li-FAU	$Li_{0.212}Na_{0.062}Ca_{0.001}Al_{0.292}Si_{0.709}O_2$	−5.24 ± 0.46	107
0.180	Na-MOR	$Na_{0.180}Al_{0.180}Si_{0.820}O_2$	−6.46 ± 0.40	96
0.256	Na-FAU	$Na_{0.256}Al_{0.256}Si_{0.744}O_2$	−22.66 ± 1.00	26
0.280	Na-FAU	$Na_{0.28}Al_{0.28}Si_{0.72}O_2$	−21.32 ± 0.59	103
0.280	Na-FAU	$Na_{0.280}Al_{0.280}Si_{0.72}O_2$	−22.06 ± 0.56	96
0.285	Na-FAU	$Na_{0.285}Al_{0.285}Si_{0.715}O_2$	−26.64 ± 1.00	26
0.444	Na-FAU	$Na_{0.444}Al_{0.444}Si_{0.556}O_2$	−41.79 ± 1.00	26
0.182	Na-HEU	$Na_{0.182}Al_{0.182}Si_{0.818}O_2$	−14.11 ± 0.45	96
0.333	Na-ANA	$Na_{0.333}Al_{0.333}Si_{0.667}O_2$	−33.82 ± 1.37	134
0.459	Na-CHA	$Na_{0.459}Al_{0.459}Si_{0.541}O_2$	−49.47 ± 15.9	103
0.182	Na-HEU	$Na_{0.098}K_{0.085}Al_{0.182}Si_{0.818}O_2$	−20.86 ± 0.74	96
0.182	Na-HEU	$Na_{0.110}K_{0.048}Ca_{0.012}Al_{0.182}Si_{0.818}O_2$	−13.43 ± 0.64	96
0.180	K-MOR	$K_{0.180}Al_{0.180}Si_{0.820}O_2$	−25.25 ± 0.57	96
0.280	K-FAU	$K_{0.26}Na_{0.02}Al_{0.28}Si_{0.72}O_2$	−48.03 ± 0.72	103
0.182	K-HEU	$K_{0.182}Al_{0.182}Si_{0.818}O_2$	−26.50 ± 0.48	96
0.200	Rb-FAU	$Rb_{0.20}Na_{0.06}Al_{0.28}Si_{0.72}O_2$	−34.34 ± 0.54	103
0.280	Cs-FAU	$Cs_{0.21}Na_{0.07}Al_{0.28}Si_{0.72}O_2$	−36.09 ± 0.46	103
0.180	Ca-MOR	$Ca_{0.090}Al_{0.180}Si_{0.820}O_2$	2.49 ± 0.40	96
0.280	Ca-FAU	$Ca_{0.14}Al_{0.28}Si_{0.72}O_2$	−3.41 ± 0.53	103
0.180	Ca-MOR	$Ca_{0.056}Na_{0.068}Al_{0.180}Si_{0.820}O_2$	−5.94 ± 0.66	96
0.333	Ca-LAU	$Ca_{0.167}Al_{0.333}Si_{0.667}O_2$	−1.26 ± 1.11	115

[a] x = Al/(Al + Si). [b] Three-letter symbol denotes zeolite structure; see ref 4.

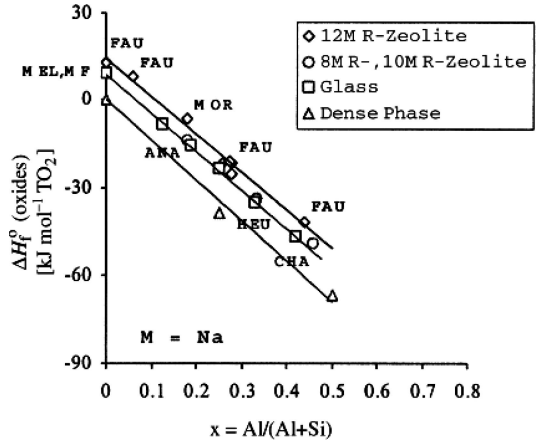

Figure 4. Enthalpies of formation at 298 K from the oxides as a function of x = Al/(Al + Si) for (a) all glasses and (b) all zeolites. Reprinted with permission from ref 96. Copyright 2001 John Wiley & Sons, Inc.

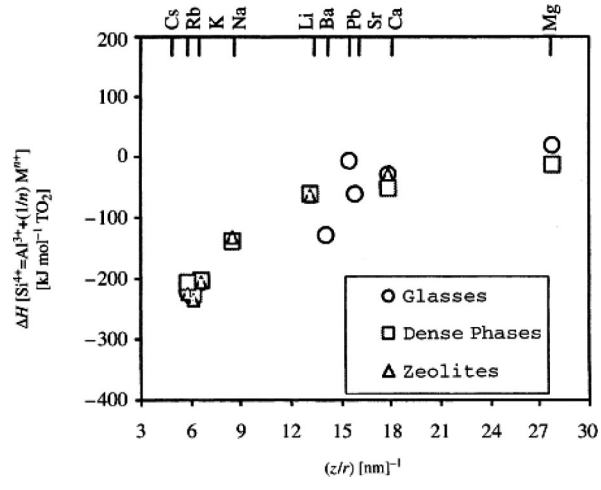

Figure 5. Enthalpies of substitution for glasses, dense phases, and zeolites as a function of the ionic potentials. Reprinted with permission from ref 96. Copyright 2001 John Wiley & Sons, Inc.

with the alkali or alkaline earth cations, those of water molecules with the walls of the cage, and, to a lesser extent, those among the water molecules themselves. In a sense, the zeolite framework is but a container to allow the most favorable possible hydration state.

Because hydration is exothermic in enthalpy but negative in entropy, such stability is limited to low temperature and hydrated zeolites usually become thermodynamically unstable with respect to dehydration and structural collapse above ~500 K. Since zeolite synthesis generally occurs under hydrothermal conditions at 300−450 K, both in nature and in the laboratory, hydrated zeolites form. The zeolite in its hydrated form is thermodynamically stable with respect to

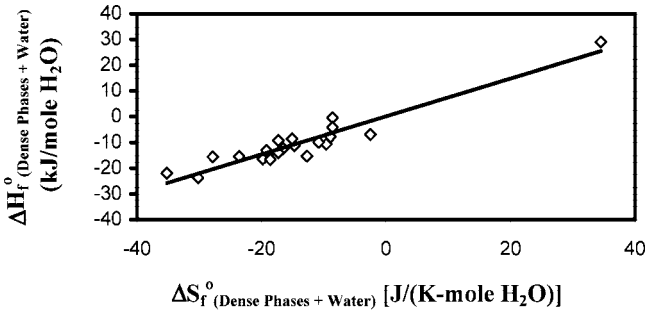

Figure 6. Enthalpy versus entropy of formation of hydrated zeolites from dense anhydrous aluminosilicates plus liquid water. Data mainly from Robie and Hemingway.[134]

the starting materials under synthesis conditions, though a particular phase may not always represent the hydrated structure of lowest free energy. Furthermore, applications to sorption, desiccation, and ion exchange often involve the hydrated forms. Thermodynamic and kinetic factors are closely intertwined in studies of hydration/dehydration, with isotherms of water content versus water fugacity showing several distinct hysteretic forms.[106]

A third generalization is the ubiquitous competition or compensation of enthalpy and entropy contributions to the thermodynamic properties. Hydration, as mentioned above, reflects a balance of favorable energetic and unfavorable entropic factors. Furthermore, their magnitudes appear correlated. Figure 6 shows that, as the enthalpy of formation becomes more negative, the entropy of formation becomes more negative. Thus, the Gibbs free energy of reaction, $\Delta G = \Delta H - T\Delta S$, represents a compensation of enthalpic and entropic factors, and ΔG varies less strongly among different zeolites than ΔH or ΔS individually.

A final generalization, or cautionary note, is that, whereas formation energetics of anhydrous zeolites from the binary oxides follow clear trends related to the aluminum content and the basicity of the extraframework cation, the energetics of hydration vary from system to system without following obvious trends related to these crystal chemical parameters, as pointed out by Yang et al.[107] This implies closely balanced competition among several factors in determining hydration energetics.

Computer simulations have been very productive in providing conceptual as well as quantitative models of both continuous and stepwise hydration. The mechanism behind continuous behavior is gradual structural rearrangement involving hydrated cations and water molecules. Simulations indicate that cation redistribution, multistep hydration of cations, and weakening of interactions between extraframework cations and the framework upon water uptake may all occur continuously for a number of zeolites including Na−zeolite Y,[65,108] NaX,[65] and Na mordenite.[58] We note also that both calculated and experimental data relevant to the energies of hydration refer to temperatures of room temperature or below (0 K for many computations), and data for hydration energies at higher temperature are unavailable. In aqueous solution, cations become more weakly hydrated and tend to associate more strongly with anions as temperature increases, but this mainly reflects change in the solvent properties of water. Since cations within zeolite cages are solvated by only a limited number of water molecules, it is reasonable to expect temperature effects on hydration energetics to be smaller.

For many other cases, numerous studies[104,105] indicate that water occupies *several distinct structural sites*, and that the water which goes on first and comes off last is held more tightly (and, hence, more exothermically) than that which comes off first and goes on last in a hydration/dehydration cycle initiated by change of temperature or water fugacity. Using computer models, energy distribution functions can be calculated and corresponding water adsorption sites can be identified, adding to the evidence of multistage sorption−desorption behavior.[64,65] Many simulations point to the existence of two kinds of water, especially in phases having large free volume such as zeolite A or Y: one being coordinated water in hydration shells of the extraframework cations and the other associated with bulklike almost free water not forming direct bonds with cations.

Several aspects of this complicated picture of hydration are directly supported by MD simulations in chabazite,[109] showing that water is strongly coordinated to Ca^{2+} at low hydration levels, while in the fully hydrated state, a large fraction of water molecules behaves as liquid water. However, one has to be cautious not to confuse energetic types of H_2O observed by thermal analysis, temperature-programmed desorption, or phase equilibria with crystallographic sites for H_2O identified in diffraction studies or computer simulations. The number of distinct types of H_2O seen in hydration energetics need not be the same as the number of distinct crystallographic sites for water molecules. For example, clinoptilolite has 5 distinct crystallographic H_2O sites, but phase equilibria reveal only one energetic type of H_2O.[110,111] Furthermore, water molecules sitting in a static fashion on preferred crystallographic sites represent a simplified picture of water ordering in zeolites. MD simulations suggest that H_2O molecules may migrate at room temperature from one preferred site to another. This is especially true for large-channel zeolites such as zeolite A in which water is shown to diffuse between α- and β- cages.[112]

Methods of high-temperature oxide melt solution calorimetry[113] now permit one to accurately elucidate energetics for a wide range of materials, and as a result, new and revised values of formation enthalpies are now available for natural and synthetic hydrated zeolites. Kiseleva at al.[114−117] studied energetics of calcium zeolites including their hydration thermodynamics. They showed that alkali substitution (Na,K) into natural leonhardite, $Ca_2Al_4Si_8O_{24}\cdot 3.5H_2O$, a partially dehydrated laumontite, decreases thermal stability (decomposition on heating in air) but increases thermodynamic stability with respect to the oxides and elements. This system is a clear case of stepwise dehydration, with equilibria among phases of stoichiometric water content, as shown in the phase diagram (Figure 7) calculated based on the thermodynamic data.[116]

Kiseleva et al.[115] also found that the integral hydration enthalpy (all values relative to liquid water) for leonhardite is −40.8 kJ/mol of H_2O and the hydration enthalpy of the most tightly bonded water is about −70 to −80 kJ/mol of H_2O. For yugawaralite, the integral hydration enthalpy is −37.5 kJ/mol of H_2O, and that of the most tightly bonded water is ∼−70 kJ/mol of H_2O. Experimental and theoretical studies[118−120] indicate that another calcium zeolite, laumontite, shows a direct correspondence between its four crystallographic H_2O sites and its four energetic types of H_2O, as evidenced by thermal analysis and water sorption experiments.

Zeolite Y is one form of the mineral zeolite faujasite (FAU), with the Si/Al ratio being 1.5−3, and is the most widely used zeolite catalyst. It is denoted as $(Ca, Mg, Na_2)_{29}$ $Al_{58}Si_{134}O_{384}H_2O_{240}$ and crystallizes in a cubic Fd3m struc-

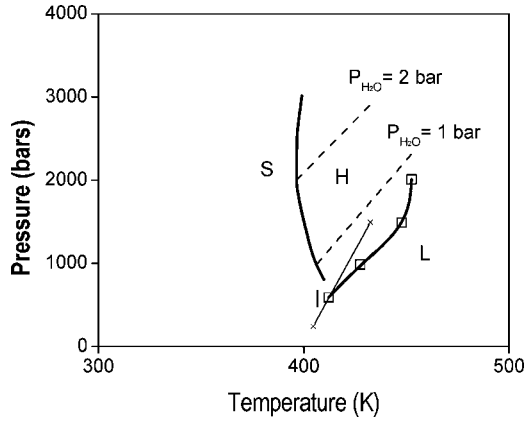

Figure 7. *P*−*T* diagram, showing the relations among stilbite (S), heulandite (H), and laumontite (L). The solid curve represents the S = H + H_2O equilibrium calculated from thermochemical data at $P_{total} = P_{H_2O}$. Dashed lines are for kbar and 2 kbar (as labeled). The light line represents the H = L + 3Q reaction (Q = quartz). The solid curve with symbols is the S = L + 3Q + H_2O equilibrium. The point "I" refers to the invariant point. Redrawn with permission from ref 116. Copyright 2001 Mineralogical Society of America.

ture.[121] Yang et al.[107] showed that energetics of various cationic forms of zeolite Y strongly depend on the exchanged cation, showing a monotonic trend of formation enthalpy against average ionic potential. The formation enthalpies of the alkali cation-exchanged zeolites can be correlated with the average ionic potential, $(Z/r)_{av}$: the zeolite tends to be more stable with increasing ionic potential. In contrast, hydration enthalpies per mole of water are roughly independent of the cation type.

Similar trends are observed in natural clinoptilolite (Cpt: $Na_{0.085}K_{0.037}Ca_{0.010}Mg_{0.020}Al_{0.182}Si_{0.818}O_2 \cdot 0.528H_2O$) and its cation-exchanged variants (Na−Cpt, NaK−Cpt, K−Cpt, and Ca−Cpt) studied by high-temperature calorimetry.[122] This zeolite occurs as massive natural deposits and can be a barrier to the migration of radionuclides in a repository such as that proposed at Yucca Mountain NV. Hydration with more efficient water−cation packing of high field strength cations is a stabilizing factor, leading to an average hydration enthalpy for all the clinoptilolites of about −30 kJ/mol of H_2O (liquid water reference state) at 298 K. The higher the average ionic potential of the extraframework cations, the larger is the hydration capacity of the clinoptilolite.[123]

The clinoptilolite system (hydrated Na−K−Ca−Al silicate) has been studied extensively by Carey and Bish.[17,124] The type of cation influences the character of the dehydration process. Both an equilibrium model[111,125] and direct calorimetric studies (by breaking an ampule of dehydrated zeolite in water in a room-temperature calorimeter)[67] suggest composition-dependent heats of hydration. The integral hydration enthalpies of Ca−Cli, Na−Cli, and K−Cli are −30.3 ± 2.0, −23.4 ± 0.6, and −22.4 ± 0.8 kJ/mol of H_2O, respectively, relative to liquid water.[125] Approaching zero water content, the regression showed the partial molar dehydration enthalpies were about −60, −48, and −45 kJ/mol of H_2O, respectively, relative to liquid water.

Chabazite (CHA) is both a mineral and a synthetic material used extensively in gas separation technology. Its hydration has been studied by several independent calorimetric investigations. Valueva and Goryanov[126] correlated the changes in Raman spectra with energetics measured by immersion calorimetry. They observed a stepwise behavior in the

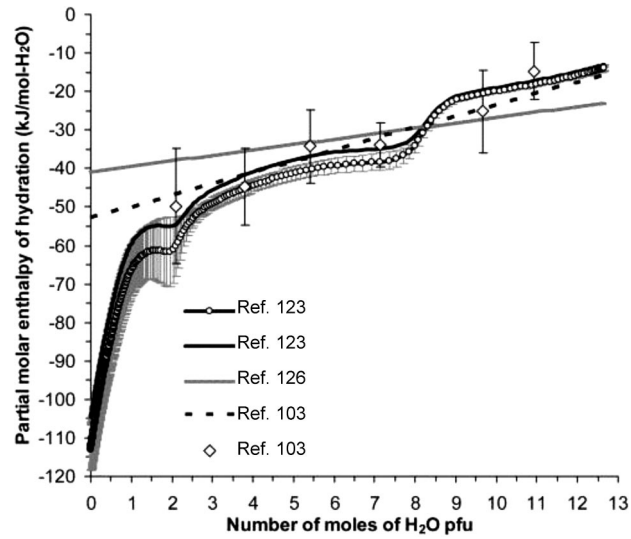

Figure 8. Partial molar enthalpy of hydration of Ca−chabazite relative to liquid water as a function of H_2O content. Reprinted with permission from ref 123. Copyright 2005 Elsevier B.V.

enthalpy of hydration of CHA as a function of H_2O content and suggested the presence of three different types of H_2O with different energetics (see Figure 8). Shim et al.[103] measured the enthalpy of Ca-exchanged CHA as a function of water content (see Figure 8). The enthalpy of removing a water molecule (partial molar enthalpy) becomes more exothermic with the degree of hydration as water content decreases from 12.5 to 0.8 molecules of water per 72-oxygen formula unit. It is also stressed in the study[103] that the enthalpy is well-fitted with a linear dependence on H_2O content. The average enthalpy of interaction of water with the zeolite is −33.4 ± 1.2 kJ/mol for Ca−chabazite and is in the same range as seen for the average value for water in Ca−leonhardite studied by Alberti.[104] In the study of Shim et al.,[103] it is also demonstrated that the experimental data by Valueva and Goryainov[126] could be represented assuming a single energetic type of H_2O. In contrast, thermodynamic analysis of phase equilibrium data by Fialips et al.[123] suggests the existence of three energetically distinct types of H_2O.

As evident from Figure 8, the Shim et al.[103] data are consistent with those of the Fialips et al.[123] work within experimental errors but are limited to higher water coverage. This emphasizes that water content resolution, kinetics of water desorption, and accuracy of energy measurements are important factors to consider when results obtained by different techniques are compared.

Zeolite Beta (BEA) is a complex intergrowth structure and has a high Si/Al ratio. A large array of cations can be exchanged into a negatively charged BEA framework, in which water is an integral part. Similar to those of other zeolites, the formation enthalpies of cation-exchanged BEA zeolite are found to be monotonic or linear functions of average ionic potential, more exothermic with increasing ionic potential (or decreasing cation size).[127]

MD simulations show[102,128] that water molecules cluster in the intersections of zeolite Beta channels and move more freely compared to those in hydrated silicalite-1 in which water molecules form small clusters (dimers, trimers) and cannot move freely. However, the presence of water may have a profound effect on the host system, resulting in altered positions and mobility of extraframework cations.[108] Such calculations are sensitive to how polarization effects are treated.[129]

Hydration enthalpies of cation-exchanged BEA determined by high-temperature oxide melt solution calorimetry[127] with Si/Al ≈ 14 (Li−BEA, Na−BEA, K−BEA, Rb−BEA, and Cs−BEA) also can be rationalized in terms of cation size or average ionic potential. The water is held energetically less tightly in this system than in more aluminum rich systems. The hydration enthalpy per mole of zeolite TO_2 decreases in magnitude in the order of decreasing average ionic potential: Li−BEA ≈ Na−BEA > K−BEA ≈ Cs−BEA > Rb−BEA. The hydration enthalpy per mole of *water* decreases in the order Li−BEA > Na−BEA > Cs−BEA > K−BEA > Rb−BEA.[127]

Similarly, the integral hydration enthalpy and formation enthalpy from oxides for a series of alkaline earth cation (Mg, Ca, Sr, Ba) exchanged zeolite Beta with Si/Al about 14 become more exothermic with increasing average ionic potential.[130] Mg−BEA and Ca−BEA have been also studied[130] and showed very endothermic formation enthalpies, in both dehydrated and hydrated forms, indicating a likely thermodynamic barrier to their direct synthesis, despite the natural occurrence of their analogue, tschernichite.

Compared to aluminosilicate analogues of similar Si/T^{3+}, the gallosilicate zeolites (Ga−NaSOD, Ga−NaFAU, Ga−NaNAT, Ga−KNAT, Ga−KLTL, and Ga−KTUN1)[131] have similar hydration enthalpy per mole of tetrahedra, but less exothermic hydration enthalpy per mole of H_2O due to higher water content of the enlarged unit cell. The hydration enthalpy per mole of water is a monotonic function of FD, whereas that per TO_2 is mainly influenced by cation type.

Along the same lines, the studies by Xu et al.[132] on several zeotypes of titanosilicates confirm a similar trend of hydration energetics: a higher level of hydration in microporous titanosilicates ETS-4 results in an increased thermodynamic stability of the framework compared to its less hydrated analogue ETS-10. Tien et al.[133] investigated the energetics of 14 synthetic manganese dioxide layered materials as well as their framework counterparts with todorokite structure. Both layered and framework materials are stabilized by hydration with diminishing stability as a function of the hydration number of the charge-balancing cations (the number of water molecules per cation). This behavior parallels that of zeolites.

Therefore, hydration of cations in the zeolite cages (which generally does not occur in the dense frameworks) can give hydrated zeolites true thermodynamic stability. In many cases, hydrated zeolites have an actual stability field at ambient conditions because their exothermic enthalpies of hydration overcome the slight metastability of the anhydrous framework with respect to dense phases plus water. Their negative enthalpies of formation from the dense aluminosilicates plus liquid water are compensated by negative entropies of formation, as exemplified in Figure 6. The energetically favorable but entropically costly interactions leading to the observed enthalpy−entropy correlation are those of water molecules with the alkali or alkaline earth cations, those of water molecules with the walls of the cage, and, to a lesser extent, those among the water molecules themselves. However, as temperature increases, the positive $T\Delta S$ of dehydration overcomes the energetic stabilization, limiting the stability field to temperatures generally less than 500 K at pressures along the vapor pressure curve of water. Thermodynamic and kinetic factors are closely intertwined in studies of hydration/dehydration, with isotherms of water content versus water fugacity showing several distinct hysteretic forms.[106]

3. Mesoporous Silica

The pursuit of larger pore sizes and more open frameworks led to discovery by Mobil scientists of a new class of porous materials, mesoporous silica (M41S).[135,136] In contrast to well-ordered zeolites, mesoporous silicas (MS) have hollow channels that are arranged in periodic arrays, while their walls are essentially amorphous. Early calorimetric studies of MCM-41 by Petrovic et al.,[137] limited to pore sizes of 2−4 nm, confirmed metastability and suggested that MS frameworks showed no dependence of energetics on pore size. Recent work by Trofymluk et al.[138] has greatly extended the type and pore size of mesoporous materials studied.[137] Two families of highly ordered mesoporous silicas, M41S (MCM-41 and MCM-48) and SBA-*n* (SBA-15 and SBA-16), were investigated in a wide range of pore sizes from 2.1 to 26.4 nm. The enthalpies observed are 19.0−31.4 kJ/mol above quartz. The cubic materials are about 4 kJ/mol less stable than those of hexagonal structure for a given pore size. The enthalpies are also raised by formation of strained rings in the amorphous walls of these materials. It is expected that the MS with larger pores are obtained at the cost of higher instability. However, an increase in pore size of more than an order of magnitude results in only 12.4 kJ/mol destabilization of framework (Table 1). This value is approximately four times the thermal energy available in a typical synthesis around 373 K. This implies that proper synthesis pathways can overcome such a moderate energy barrier. It was mentioned above that the formation enthalpy of zeolites has a strong correlation with FD or MV, as denser frameworks possess more stable structures relative to less dense polymorphs. Here, in the same fashion, MS with higher pore volume are less stable. Figure 2 shows the formation enthalpy versus MV for the MS studied along with the data for zeolites. MV is calculated by adding the molar pore volume from the Kruk−Jaroniec−Sayari[139,140] method and MV of amorphous silica. MS data seem to follow the general trend for zeolites, though significant scatter is observed, possibly due to higher uncertainty in pore volume measurements and unaccounted variations of MS density.

4. Interactions with Structure-Directing Agents

The studies outlined in the above sections (and also discussed below) have shown that energetics depend only weakly on the framework type for a variety of isocompositional microporous materials (silica zeolites, aluminum phosphates, selected aluminosilicates, and manganese oxide octahedral microporous frameworks[141]). When a given structure crystallizes under the influence of a template or structure-directing agent (SDA) such as a tetraalkylammonium cation, what is the role of the SDA? Is it purely stereochemical (kinetic and entropic) in nature, or do differences in the energetics of interaction of the SDA with the framework play a role, even though the final calcined products are similar in energy?

Davis and Lobo[23] put forward a classification of zeolite templates that attempted to distinguish them by their roles in zeolite synthesis. This classification emphasizes the observation that some frameworks are obtained by a specific SDA, and its use truly leads to the framework of unique geometric and electronic properties, while others can be

synthesized by the use of different templates. Some templates such as amines, which result in many framework structures, act as "space fillers" and, although stabilizing the pores, display a nonspecific relationship with products.[142,143] The diversity in frameworks formed is achieved through molecular flexibility that permits a template to adopt different configurations in order to fit voids of various shapes.[144,145] All this reinforces the findings reviewed in previous sections. The energetics of framework formation are closely balanced, resulting from a set of intertwined interactions at the interface between the framework, SDA, and water. Figure 10 shows how small energy terms all compete in energy landscape to yield different local minima and different pathways and products.

It is important to stress that a geometrical match between zeolite voids and SDA is a necessary condition to a successful synthesis of a particular framework.[146−148] In some cases, the symmetry match between the zeolite framework and SDA is quite remarkable.[149] The molecular mechanism underpinning templating is the following. Template molecules maximize the short-range nonbonding interactions with the framework, thus increasing stability of the resultant structure.[2] Among many similar SDAs, only ones with appropriate hydrophobicity/hydrophilicity can be used, limiting the C/N ratio to 11−16.[24] However, there are some synthetic routes designed rather to do the opposite: a "geometrical mismatch" between the strongly interacting template admixed in small amounts into the solution of the major SDA and the framework suppresses its formation, leading to a new zeolite structure (structure-blocking mechanism).[150]

Piccione et al.[151] studied the interaction of four frameworks (BEA, MFI, MTW, and STF) with some of four SDA molecules TEA, TPA, BISPIP, and SPIRO, the last two being large nitrogen-containing molecules with aromatic or cyclic moieties, by HF solution calorimetry. The interactions (per mole of silica) are small (between −1 and −6 kJ/mol of TO_2), and the ΔH and $T\Delta S$ terms are similar. The ΔH values were measured directly, while the $T\Delta S$ term was estimated. The authors inferred that there is no energetic correlation between framework geometry and density or with whether the SDA specifically templates only one structure or can be used in the synthesis of several different zeolites. These findings imply the absence of strong specific interaction of SDA and the corresponding framework. The results suggest that the templates play a kinetic, rather than thermodynamic, role in selecting a particular structure among many other configurations of similar energy. Throughout the nucleation and crystallization stages, a balance between thermodynamic and kinetic factors governs the outcome of a particular synthesis. Computer simulations confirm these findings. For example, Sastre et al.[152] demonstrated that the stabilization of intermediate species during nucleation is important to directing the final product.

To test whether the structure of the matrix affects the interactions of SDAs with mesoporous silica, Trofymluk at al. (unpublished) measured the enthalpies of solution for a series of pure mesoporous materials (MCM-41, MCM-48, SBA-15, and SBA-16) in their as-made and calcined forms by HF calorimetry at 323 K. The interaction enthalpies of organic SDAs and inorganic hosts were calculated by taking the difference between the enthalpies of solution for the as-made and calcined materials. The enthalpies of interaction span a narrow exothermic range of −6.0 to −19.6 kJ/mol of SiO_2, all not more negative than $-2RT$, the thermal energy. This explains why many SDAs can direct mesoporous silica synthesis toward several structures.

Much effort has been put into computer studies aimed at predicting energetically stable SDA−framework combinations using molecular mechanics.[142,143,153] The calorimetric studies explored energetics in systems in which an SDA is successfully used to synthesize framework materials and, thus, a good geometric match is inherent. In addition, computational methods have proved very useful in identifying SDA candidates for the synthesis of prospective frameworks. For example, molecular mechanics was employed by Schmitt and Kennedy[147] to rationally design and screen new template molecules for zeolite ZSM-18 (MEI). Their work predicted the geometries for a range of candidate templates. These molecules were then screened by inspecting the van der Waals overlap produced when the optimized template was placed insight the zeolite cage. The derivation of new templates for this framework was a notable success because, prior to this study, there was only one template known to synthesize ZSM-18. Moreover, the best template derived from this work had the benefit that it could be more easily removed from the framework, resulting in reduced loss of crystallinity in the product on calcination. The molecular graphics approach has been widely used to place optimized templates into the framework structure, as in the case of the EUO structure.[154] This demonstrated the excellent void-filling properties exhibited by organic SDAs that successfully template this framework. New templates and structures (for example, 4-piperidinopiperidine for DAF-5, a CoAPO material) were successfully designed using a technique based on computational "growth" of a template molecule inside the zeolite host from a fragment database maximizing a number of template−host contacts.[153,155,156] Yet, as calorimetry has shown, such templating involves very small energetic advantages and is indeed largely a geometric effect.

5. Zeotypes

In addition to aluminosilicates and pure silica microporous materials, frameworks bearing features of zeolite structures occur for many other compositions. Aluminophosphate $AlPO_4$ materials are an example of an important class of zeolite-type, zeotype, materials.

Hu et al.[71] demonstrated that the enthalpies of a series of $AlPO_4$ ($Al_{0.5}P_{0.5}O_2$ on two oxygen basis) cluster in a small range relative to berlinite (the stable quartz form of $AlPO_4$), forming an energy landscape with even smaller metastability (11.5−16.7 kJ/mol of TO_2) than that for pure silica materials relative to quartz. The enthalpies of formation for $AlPO_4$-type zeolites show a nonlinear dependence on MV as seen in Figure 2. Small amounts of water, present in the as-synthesized samples, help stabilize the framework, resulting in negative heats of formation from berlinite plus liquid water. It also has been proposed[71] that the enthalpy may level off at a value about 8−10 kJ/mol above berlinite. No large pore materials of this type have been measured so far, and the current data set is restricted. However, the data clearly indicate the accessibility of a large number of structures of very similar energies, and similar trends are observed as in pure-silica zeolites.

Templating with amines produces even more open phosphate frameworks in which the organics and fluorine play an integral part, and unusual coordinations and broken rings are sometimes present.[157,158] Gerardin et al. conducted a

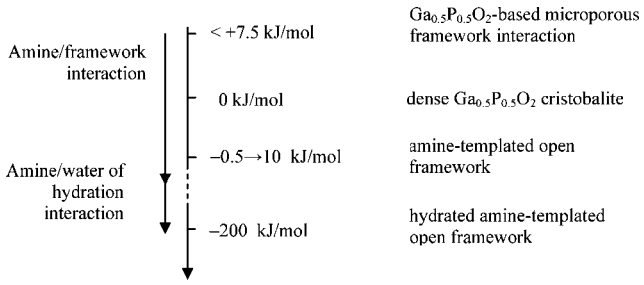

Figure 9. Schematic showing the metastabilily of ULM-*n* samples with the orders of magnitude of interaction energies involved in the hybrid materials (data from ref 159).

calorimetric study[159] on some gallophosphate ($GaPO_4$ or $Ga_{0.5}P_{0.5}O_2$ on two oxygen basis) ULM-*n* phases. The observed energetics are shown schematically in Figure 9. The "dry" $GaPO_4$ framework is metastable with respect to the dense cristobalite form of $GaPO_4$ by 5−7.5 kJ/mol of $P_{0.5}O_2$. The amine-containing (diaminopropane or diaminohexane) zeolite is stable by 0.5−5 kJ/mol. Also, an interaction enthalpy of less than −25 kJ/mol, typical for framework−guest interactions, is in good agreement with what is known for hydrogen bonds (~10 kT/molecule). However when water enters the same cage as the amine, the stabilization increases to as much as 100 kJ/mol, comparable to energies of hydration of amines in water. Thus, the enthalpies of amine-templating are small, forming a competitive energy landscape for different structures, but, once water can complex with the amine, much higher stability is gained. One suspects that this large stabilization in energy is compensated by a corresponding loss of entropy (tighter bonding and loss of motional freedom).

The picture becomes even more complicated when additional species compete for the available sites in the framework pores. The enthalpy of formation of cancrinite from oxides becomes less exothermic and the water content decreases with increasing salt inclusion ($NaNO_3$ and Na_2CO_3), indicating the destabilizing effects of "imbibed" (absorbed) salt.[160] This implies a competition between water molecules, guest anions, and possibly Na cations for the occupancy of the cancrinite 12-membered ring channel and cage sites.

Framework cations, which favor different bonding geometries, may significantly modify the local framework structure and energy landscape. For example, substitution of germanium into silica zeolite structures results in smaller T−O−T angles.[83]

Corma et al.[161−163] synthesized a series of new large-pore tridirectional (Si,Ge)-zeolites (called the ITQ series) by combining appropriate organic SDAs and framework isomorphic substitution of germanium for silicon. ITQ-7 is structurally related to zeolite Beta, while ITQ-21 contains cavities as spacious as those of FAU but interconnected through six 12-MR pores of 0.74 nm.[163]

Calorimetric studies by Li et al.[164,165] on a series of Ge-containing zeolites synthesized by the Corma group show that these phases become increasingly metastable with respect to a mixture of the quartz forms of SiO_2 and GeO_2 with increasing Ge content, which corresponds to decreasing FD or increasing MV. The slope of the line relating enthalpy to volume or the extent of Ge-substitution varies from one family of Ge-containing zeolites to another. The preferential substitution of Ge in "double four rings" (which seldom exist for silica materials) is reflected in diminished metastability.[83]

Table 3. Energetics of Microporous Transition Metal Phosphates

composition	F.D.	formation enthalpy from binary oxides, kJ/mol	ref
Alpha $NaCoPO_4$	28.1	−349.7 ± 2.3	169
Beta $NaCoPO_4$	26.3	−332.1 ± 2.5	169
$NaH(ZnPO_4)_2$		−515.5 ± 2.7	170
$NaZnPO_4$	20.7	−339.6 ± 2.6	170
$NaZnPO_4 \cdot H_2O$	16.7	−346.9 ± 2.4	171
$Na_6(ZnPO_4)_6 \cdot 8H_2O$	17.3	−344.7 ± 2.4	172
$NaCo_{0.3}Zn_{0.7}\ PO_4 \cdot 4/3H_2O$		−344.1 ± 2.4	170
α-$KCoPO_4$		−375.8 ± 2.5	173
γ-$KCoPO_4$		−376.9 ± 1.8	173
$RbCoPO_4$		−381.4 ± 4.8	173
α-$Cu_2P_2O_7$		−279.0 ± 1.4	174
$Cu_3(P_2O_6OH)_2$		−538.0 ± 2.7	174

A similar trend in substitution−structure relationships is observed in frameworks containing d-electron ions, particularly Ni, Co, and Zn, capable of tetrahedral coordination. Their larger size and weaker bonding lead to the possibility of smaller T−O−T angles, which in turn favor a wider distribution of angles needed to stabilize larger cages.[166] These ions substitute into $AlPO_4$-based materials, but end-member transition metal phosphate microporous materials, with and without organics, are also known.

Le et al.[167,168] studied phosphate framework materials containing transition metals Co, Ni, or Zn with or without extra water and hydroxyl, and with and without Na as a channel cation. These show framework densities ranging from 16 to 28, structures ranging from conventional zeolites to mixed octahedral−tetrahedral frameworks, and varying alkali and water contents. Alkali and ammonium cobalt and zinc phosphates show rich polymorphism.

Acid−base interactions dominate the energetic trends in these phosphates systems: stronger acid−base interactions than in aluminosilicates result in more exothermic formation enthalpies from oxides.

$$1/2A_2O\ (cr, 298\ K) + CoO\ (cr, 298\ K) + 1/2P_2O_5\ (cr, 298\ K) \rightarrow ACoPO_4\ (cr, 298\ K) \quad (5)$$

Co and Zn phosphates exhibit similar trends in enthalpies of formation from oxides as aluminosilicates, but their enthalpies of formation from oxides are more exothermic because of their stronger acid−base interactions (see Table 3). CoO and ZnO are oxides of similar basicity, resulting in similar enthalpies of formation for NH_4CoPO_4 and NH_4ZnPO_4 and for $NaZnPO_4$ and $NaCoPO_4$ from constituent ammonia and oxides.

6. Synthesis and Transformations of Zeolites and Related Materials

The hydrothermal synthesis of zeolites is still a largely empirical science, with the choice of reagents (forms of silica and alumina), concentrations of reagents, structure-directing agent, temperatures and/or heating rate, and duration of runs optimized by trial and error. Although the aqueous phase and amorphous and nanoscale particles in it presumably evolve continuously, the actual appearance of a crystalline product often occurs over a fairly short time segment, and "overcooking" the reaction mixture may lead to undesirable products. Clearly a number of competing reaction pathways is possible, and the products formed represent a competition

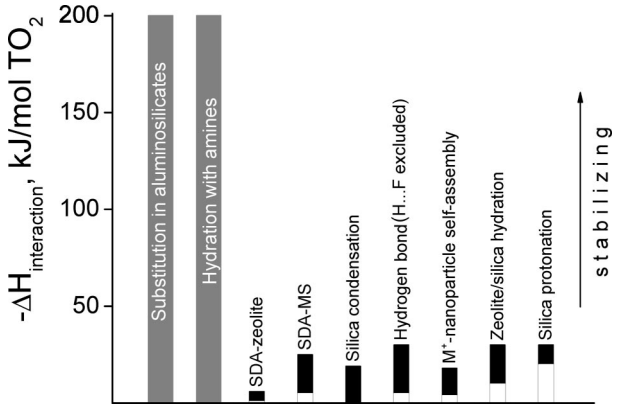

Figure 10. Energetics of interactions involved in the synthesis of microporous and mesoporous materials. Data are taken from a number of sources[14,151,159,176−179,195] and summarized in ref 175. Bands show the range of interaction enthalpies.

among thermodynamic and kinetic factors. The literature on zeolite synthesis is extensive and largely beyond the scope of the present review, but the reader is referred to several comprehensive reviews[1−3,6−14] of the topic. Here we stress only some thermodynamic or at least energetic factors in illustrating the usefulness of calorimetry as a probe of the synthesis process.

Figure 10 illustrates the magnitudes of various interactions involved in zeolite synthesis. The most exothermic interactions involve the formation of alkali or alkaline earth aluminosilicate condensed structures from dissolved aqueous ions and the hydration of amines, if present. Once gels, nanoparticles, or amorphous phases have formed, the remaining interactions typically have enthalpies of less than 50 kJ/mol of tetrahedra, as shown in the right-hand part of Figure 10.[175] A similar argument can be made in terms of free energies. The small magnitude of and competition among these various interactions sets the stage for competitive self-assembly.

The growth of silicalite (MFI) from an initially clear solution of silica, which, however, contains nanoparticles of suboptical dimensions, offers an interesting case study of the interplay of thermodynamic and kinetic factors. MFI silica zeolite (silicalite-1) is the only zeolitic system in which crystal growth from nanoparticle precursors is well-documented.[14,176−182] Silicalite-1 is unique in many other aspects, such as synthesis simplicity, reduced number of constituents, and formation from clear sol solutions, all making it a very useful model system. It is synthesized from clear solutions or sols that consist of a silica source (usually tetraethylorthosilicate $Si(OC_2H_3)_4$ or TEOS), tetrapropylammonium hydroxide (TPAOH) as SDA, and water. Formation of nanoparticles of 5 nm or less in size occurs immediately after TEOS hydrolysis.[14,176−179] There is an ongoing debate as to what role these nanoparticles play in zeolite synthesis.[183] The central question is whether precursor nanoparticles are building units from which larger single crystals are assembled by attachment like Lego blocks (aggregation mechanism),[184−189] or whether they are just a "packed" raw material supplying silica monomers and oligomers to growing nuclei.[176,190] The former assumes that there exists a mechanism by which the nanoparticles coalesce to form larger single crystals. The latter involves dissolution or release of species into solution before they become part of larger crystals. Aggregation may involve oriented attachment of the particles.[191,192] One has to be careful as observations by microscopic methods of the

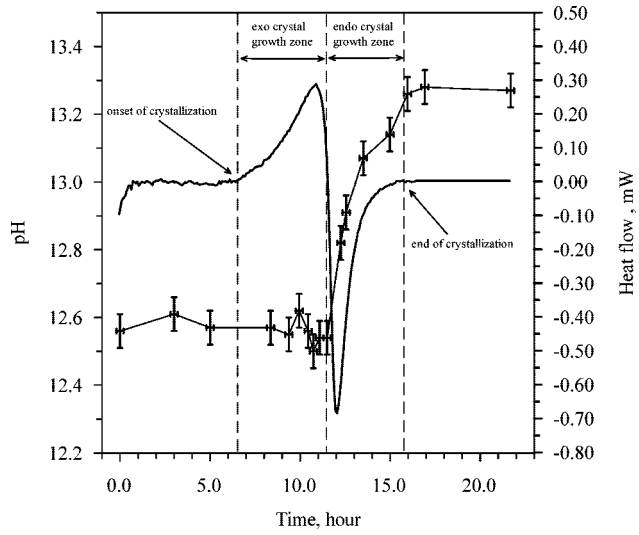

Figure 11. Evolution of enthalpy and solution pH during MFI templated synthesis. Reprinted with permission from ref 193. Copyright 2002 American Chemical Society.

"aggregated" nanoparticles in zeolite crystal growth experiments may be misleading.[192] What is observed may result from growth processes that do not occur by the aggregation mechanism at all or may reflect changes when the samples are removed from solution, dried, or exposed to vacuum.

In this context, in situ scanning calorimetry in a closed chemical system is an essential tool to elucidate the energetics and kinetics of zeolite formation. Yang et al.[193,194] used a Calvet calorimeter to study the synthesis of silicalite-1 from an initially clear solution containing the silica source and a tetrapropylammonium (TPA) salt as SDA. The initial hydrolysis of the silica source in the presence of TPA proceeds rapidly, resulting in a clear ethanol−water solution having particles 3 nm in size. On the basis of calorimetric and structural data, Yang et al.[193,194] suggested that these nanoparticles bear some structural features of the zeolite-to-be. In situ calorimetry, combined with mass balance studies, pH measurements, and ^{29}Si NMR studies, suggests the following sequence of steps upon heating. Figure 11 shows the initial exothermic process with a modest heat effect of −2 kJ/mol of SiO_2 zeolite formed. This is followed by an endothermic step with 2.5 kJ/mol, leading to a total enthalpy of 0.5 kJ/mol.

In the exothermic stage, the amount of zeolite formed and the heat released are linear with time, while the solution pH remains constant. After 50−70% completion, the zeolite-forming exothermic reaction slows, the enthalpy becomes endothermic, and the pH rises. The initial exothermic stage with linear rate law and constant pH probably involves the attachment of the 3 nm organic-containing nanoparticles onto the growing crystal. Since the reaction occurs at pH 9, or higher, both the crystal and the nanoparticles are negatively charged. Since the pH stays constant, this stage of synthesis must involve the localization of these hydroxyls onto a surface that is decreasing in area. Eventually, the buildup of surface charge becomes thermodynamically unfavorable, the particles and growing crystal repel each other too strongly, and the reaction slows. Further reaction can only occur accompanied by the release of OH^-, H_2O, and/or organics into solution, raising the pH. This release of hydroxyl is endothermic in energy but driven by entropy; thus, the switch to a net endothermic enthalpy occurs.

Rimer et al.[14] put forward ideas that interpret zeolite growth from clear solutions in terms of self-assembly of molecular aggregates, based on a concept of pseudophase separation of SDA and silica precursor. The acid−base chemistry of silanol groups is at the heart of their formulation. They infer that the silica nanoparticles in clear solutions of SDA and silica have a core−shell structure with silica mainly in the core and the organic cations largely in the shell. Heating under hydrothermal conditions acts upon solutions that contain mostly segregated organic cations and silica at room temperature, leading to the organic cations being embedded within the pores at synthesis temperature. In this process, core−shell silica particles are transformed into zeolite on the growing surface, but it is not clear how much of the transformation takes place in the particles and how much is mediated by species in solution. This transformation triggers and directs the structure evolution in silica, whereby the size and geometry of the organic cation induce changes in the structure leading to zeolite.

Rimer et al.[195] used calorimetry to follow a series of reactions associated with silica nanoparticle formation upon adding a silica source, TEOS, into basic solution of a monovalent cation. Heat attributed to self-assembly of nanoparticles at a critical silica concentration was measured and found to be independent of alkalinity, but varying with cation type. Nanoparticle formation from silicate species has been shown to involve endothermic reactions, derived from protonation of negatively charged silica to form neutral species, which participate in condensation, thereby providing an explanation for the previously observed exothermic−endothermic crossover as a function of time during syntheses.

Rimer et al.[179] also employed complementary small-angle X-ray scattering (SAXS) and microcalorimetry to study the dissolution of silica nanoparticles that serve as precursors in the synthesis of silicalite-1. The nanoparticle dissolution rates and enthalpies decrease in magnitude toward those of silicalite-1, implying that a structural reorganization of silica, organics, and H_2O within the particles occurs during zeolite growth. The silica nanoparticles were found to be amorphous, though more ordered than those in dense amorphous silica, and to structurally reorganize with increasing time of heat treatment.

Solution-mediated transformations of zeolites are important pathways to create new framework materials. Lamellar structures are often observed as intermediate phases during zeolite synthesis.[196,197] However, a reaction overrun in which the zeolite product decomposes to form denser phases is a common phenomenon, reflecting the metastability of microporous materials, is widely exploited in the zeolite synthesis.[2] In this sense, aluminous open framework systems such as zeolite A and X decompose into sodalite, whereas siliceous zeolites transform to quartz or cristobalite.[2,198−200] Gross et al.[201] used in situ scanning microcalorimetry to study thermodynamics of the hexagonal-to-lamellar phase transition in silica−surfactant nanocomposites. Thermal events in the calorimetric experiments were directly linked to the rearrangement of the organic template molecules and changes in chemistry of the inorganic framework. In order to separate these contributions, calorimetric data were collected during heating in water, where a hexagonal-to-lamellar phase transition takes place, and in an acidic buffer, where no phase change occurs. An endotherm near 70 °C in all samples was attributed to an order−disorder transformation of the organic surfactant. Two endotherms observed for the water-treated composites were assigned to the hexagonal-to-lamellar phase transformation, which has an enthalpy of $+0.5 \pm 0.1$ kJ/mol of SiO_2 or $+2.4 \pm 0.3$ kJ/mol of surfactant and an entropy change of $+1$ J K^{-1} mol^{-1} of SiO_2 or $+6$ J K^{-1} mol^{-1} of surfactant. This endothermic effect implies that rearrangement to the more open lamellar phase is entropy-driven, in line with confinement effects of the organic molecules. It also confirms that the hexagonal phase is thermodynamically stable at low temperature and the lamellar phase is stable at high temperature.

Liu et al.[202] followed, using in situ calorimetry, the formation of nitrate sodalite, an important product at DOE nuclear waste storage sites. Despite solid evidence for a transition sequence of amorphous-zeolite A−sodalite−cancrinite, no calorimetric peak of the zeolite A to sodalite conversion was observed, suggesting a very low transition enthalpy (<1 kJ/mol of TO_2).

Taking advantage of improvements in computational methods in the past few years, DFT and Monte Carlo methods have been used intensively to explore zeolite synthesis and particle growth. These studies support the findings by experimental methods (NMR, X-ray and neutron scattering, adsorption, thermogravimetric analysis, and calorimetry) that, at early states of zeolite growth, amorphous nanoparticles exist and act as seeds for zeolite growth occurring through crystallization and Ostwald ripening.[14,203]

In this context, amorphous silica is an important model for studies of surface chemistry, synthesis, and stability, for both microporous and mesoporous materials. There have been many studies devoted to stability of strained rings, ring-size distribution, bond and angle configurations, and catalytic properties of the silica surface, its hydration, and water dissociation; the reader is referred to these works.[204−209]

7. Concluding Remarks

The thermodynamics of zeolites, zeolite-related frameworks, and mesoporous silicas reflect a rich and closely balanced energy landscape of competing energetic and entropic factors. The complex pathways of zeolite formation, hydration, and transformation are made possible by small differences in thermodynamic driving forces for competing reactions, upon which are superimposed various kinetic barriers and mechanistic constraints. Anhydrous zeolitic frameworks are metastable with respect to dense phases by less than 15 kJ/mol of tetrahedra in most cases, with mesoporous silicas metastable by 15−30 kJ/mol. The magnitude of this energetic difference increases with increasing molar volume (decreasing framework density). The energetics of formation of anhydrous aluminosilicate zeolites varies linearly with the aluminum content and parallels the energetics of glass formation for aluminosilicates with the same monovalent or divalent cation. The entropy of silica zeolites is not a strong function of their density, reflecting the strong bonding in the tetrahedral framework and, presumably, similar vibrational density of states. Thus, the enthalpy is the main factor in determining the stability of different framework topologies at the same composition.

Many hydrated aluminosilicate zeolites can have a thermodynamic stability field near room temperature, indicating that the exothermic enthalpy of hydration more than compensates for the metastability of the anhydrous framework. However, the large positive entropy of dehydration limits zeolite stability to temperatures below 400−500 K. The details of hydration energetics are complex and differ for

various structures, but in general, the enthalpy of hydration becomes less exothermic with increasing water content.

The enthalpies and entropies of interaction of structure-directing agents with the zeolite framework also reflect closely balanced small enthalpy and entropy factors. This sets the stage for complex and competing mechanisms of zeolite formation and transformation during zeolite synthesis. In particular, the role of nanoparticles in zeolite synthesis is an area of current interest and controversy. Structural, mechanistic, and calorimetric studies, especially during early stages of zeolite synthesis, offer a path forward to a comprehensive picture of the complex interactions of silica (in solution, oligomers, nanoparticles, and solid phases) with the aqueous phase and with organic and inorganic additives during hydrothermal synthesis.

8. References

(1) Cundy, C. S.; Cox, P. A. *Chem. Rev.* **2003**, *103*, 663.
(2) Cundy, C. S.; Cox, P. A. *Microporous Mesoporous Mater.* **2005**, *82*, 1.
(3) Smith, J. V. *Chem. Rev.* **1988**, *88*, 149.
(4) Baerlocher, C.; Meier, W. M.; Olson, D. H. *Atlas of zeolite framework types*; Elsevier: Amsterdam, The Netherlands, 2001.
(5) Baerlocher, C.; McCusker, L. B.; Olson, D. H. *Atlas of Zeolite Framework Types*, 6th ed.; Elsevier: Amsterdam, The Netherlands, 2007.
(6) Corma, A. *Chem. Rev.* **1997**, *97*, 2373.
(7) Taguchi, A.; Schuth, F. *Microporous Mesoporous Mater.* **2005**, *77*, 1.
(8) Corma, A.; Davis, M. E. *ChemPhysChem* **2004**, *5*, 304.
(9) Davis, M. E. *Nature* **2002**, *417*, 813.
(10) Sefcik, J.; McCormick, A. V. *AIChE J.* **1997**, *43*, 2773.
(11) Sefcik, J.; McCormick, A. V. *Chem. Eng. Sci.* **1999**, *54*, 3513.
(12) Kragten, D. D.; Fedeyko, J. M.; Sawant, K. R.; Rimer, J. D.; Vlachos, D. G.; Lobo, R. F.; Tsapatsis, M. *J. Phys. Chem. B* **2003**, *107*, 10006.
(13) Fedeyko, J. M.; Rimer, J. D.; Lobo, R. F.; Vlachos, D. G. *J. Phys. Chem. B* **2004**, *108*, 12271.
(14) Rimer, J. D.; Fedeyko, J. M.; Vlachos, D. G.; Lobo, R. F. *Chem.—Eur. J.* **2006**, *12*, 2926.
(15) Sastre, G. *Phys. Chem. Chem. Phys.* **2007**, *9*, 1052.
(16) Yu, J. H.; Xu, R. R. *Chem. Soc. Rev.* **2006**, *35*, 593.
(17) Bish, D. L.; Carey, J. W. In *Natural Zeolites: Occurrence, Properties, Applications*; Mineralogical Society of America and the Geochemical Society: Washington, D.C.; 2009; Vol. 45.
(18) Bekkum, H. v. *Introduction to zeolite science and practice*, 2nd ed.; Elsevier: Amsterdam, New York, 2001.
(19) McCusker, L. B.; Liebau, F.; Engelhardt, G. *Pure Appl. Chem.* **2001**, *73*, 381.
(20) Suib, S. L. *Chem. Rev.* **1993**, *93*, 803.
(21) Occelli, M. L.; Kessler, H. *Synthesis of porous materials: Zeolites, clays, and nanostructures*; Marcel Dekker: New York, 1997.
(22) Freyhardt, C. C.; Tsapatsis, M.; Lobo, R. F.; Balkus, K. J.; Davis, M. E. *Nature* **1996**, *381*, 295.
(23) Davis, M. E.; Lobo, R. F. *Chem. Mater.* **1992**, *4*, 756.
(24) Burton, A. W.; Zones, S. I.; Elomari, S. *Curr. Opin. Colloid Interface Sci.* **2005**, *10*, 211.
(25) Petrovic, I.; Heaney, P. J.; Navrotsky, A. *Phys. Chem. Miner.* **1996**, *23*, 119.
(26) Petrovic, I.; Navrotsky, A. *Microporous Mater.* **1997**, *9*, 1.
(27) Piccione, P. M.; Laberty, C.; Yang, S. Y.; Camblor, M. A.; Navrotsky, A.; Davis, M. E. *J. Phys. Chem. B* **2000**, *104*, 10001.
(28) Piccione, P. M.; Woodfield, B. F.; Boerio-Goates, J.; Navrotsky, A.; Davis, M. E. *J. Phys. Chem. B* **2001**, *105*, 6025.
(29) Piccione, P. M.; Yang, S. Y.; Navrotsky, A.; Davis, M. E. *J. Phys. Chem. B* **2002**, *106*, 5312.
(30) Mokaya, R. *J. Phys. Chem. B* **1999**, *103*, 10204.
(31) Cassiers, K.; Linssen, T.; Mathieu, M.; Benjelloun, M.; Schrijnemakers, K.; Van Der Voort, P.; Cool, P.; Vansant, E. F. *Chem. Mater.* **2002**, *14*, 2317.
(32) Zhao, D. Y.; Feng, J. L.; Huo, Q. S.; Melosh, N.; Fredrickson, G. H.; Chmelka, B. F.; Stucky, G. D. *Science* **1998**, *279*, 548.
(33) Zhao, D. Y.; Huo, Q. S.; Feng, J. L.; Chmelka, B. F.; Stucky, G. D. *J. Am. Chem. Soc.* **1998**, *120*, 6024.
(34) Han, Y. J.; Stucky, G. D.; Butler, A. *J. Am. Chem. Soc.* **1999**, *121*, 9897.
(35) Wang, S.; Choi, D. G.; Yang, S. M. *Adv. Mater.* **2002**, *14*, 1311.
(36) Lauffer, R. B. *Chem. Rev.* **1987**, *87*, 901.
(37) Ihlein, G.; Junges, B.; Junges, U.; Laeri, F.; Schuth, F.; Vietze, U. *Appl. Organomet. Chem.* **1998**, *12*, 305.
(38) Han, Y. J.; Kim, J. M.; Stucky, G. D. *Chem. Mater.* **2000**, *12*, 2068.
(39) Ryoo, R.; Ko, C. H.; Kruk, M.; Antochshuk, V.; Jaroniec, M. *J. Phys. Chem. B* **2000**, *104*, 11465.
(40) Huang, M. H.; Choudrey, A.; Yang, P. D. *Chem. Commun.* **2000**, 1063.
(41) Tanev, P. T.; Pinnavaia, T. J. *Chem. Mater.* **1996**, *8*, 2068.
(42) Bruinsma, P. J.; Kim, A. Y.; Liu, J.; Baskaran, S. *Chem. Mater.* **1997**, *9*, 2507.
(43) Parmentier, J.; Saadhallah, S.; Reda, M.; Gibot, P.; Roux, M.; Vidal, L.; Vix-Guterl, C.; Patarin, J. *J. Phys. Chem. Solids* **2004**, *65*, 139.
(44) Van Santen, R. A.; Offermans, W. K.; Malek, K.; Pidko, E. A. *Mol. Simul.* **2007**, *33*, 327.
(45) Filippone, F.; Buda, F.; Iarlori, S.; Moretti, G.; Porta, P. *J. Phys. Chem.* **1995**, *99*, 12883.
(46) Shannon, S. R.; Campbell, B. J.; Metiu, H.; Blake, N. P. *J. Chem. Phys.* **2000**, *113*, 10215.
(47) Moloy, E. C.; Cygan, R. T.; Bonhomme, F.; Teter, D. M.; Navrotsky, A. *Chem. Mater.* **2004**, *16*, 2121.
(48) Camblor, M. A.; Diaz-Cabanas, M. J.; Cox, P. A.; Shannon, I. J.; Wright, P. A.; Morris, R. E. *Chem. Mater.* **1999**, *11*, 2878.
(49) Hafner, J.; Benco, L.; Bucko, T. *Top. Catal.* **2006**, *37*, 41.
(50) Schwarz, K.; Nusterer, E.; Margl, P. *Int. J. Quant. Chem.* **1997**, *61*, 369.
(51) Shah, R.; Gale, J. D.; Payne, M. C. *J. Phys. Chem.* **1996**, *100*, 11688.
(52) Shah, R.; Payne, M. C.; Lee, M. H.; Gale, J. D. *Science* **1996**, *271*, 1395.
(53) Bougeard, D.; Smirnov, K. S. *Phys. Chem. Chem. Phys.* **2007**, *9*, 226.
(54) Chatterjee, A.; Mizukami, F. *Chem. Phys. Lett.* **2004**, *385*, 20.
(55) Pedone, A.; Malavasi, G.; Menziani, M. C.; Segre, U.; Musso, F.; Como, M.; Civalleri, B.; Ugliengo, P. *Chem. Mater.* **2008**, *20*, 2522.
(56) Fois, E.; Gamba, A.; Tabacchi, G. *J. Phys. Chem. B* **1998**, *102*, 3974.
(57) Bolis, V.; Busco, C.; Ugliengo, P. *J. Phys. Chem. B* **2006**, *110*, 14849.
(58) Maurin, G.; Bell, R. G.; Devautour, S.; Henn, F.; Giuntini, J. C. *J. Phys. Chem. B* **2004**, *108*, 3739.
(59) Poulet, G.; Sautet, P.; Tuel, A. *J. Phys. Chem. B* **2002**, *106*, 8599.
(60) Beauvais, C.; Boutin, A.; Fuchs, A. H. *Cr. Chim.* **2005**, *8*, 485.
(61) Hill, J. R.; Freeman, C. R.; Delley, B. *J. Phys. Chem. A* **1999**, *103*, 3772.
(62) Sefcik, J.; Demiralp, E.; Cagin, T.; Goddard, W. A. *J. Comput. Chem.* **2002**, *23*, 1507.
(63) Higgins, F. M.; Leeuw, N. H. d.; Parker, S. C. *J. Mater. Chem.* **2002**, *12*, 124.
(64) Di Lella, A.; Desbiens, N.; Boutin, A.; Demachy, I.; Ungerer, P.; Bellat, J. P.; Fuchs, A. H. *Phys. Chem. Chem. Phys.* **2006**, *8*, 5396.
(65) Shirono, K.; Endo, A.; Daiguji, H. *J. Phys. Chem. B* **2005**, *109*, 3446.
(66) Hill, J. R.; Stuart, J. A.; Minihan, A. R.; Wimmer, E.; Adams, C. J. *Phys. Chem. Chem. Phys.* **2000**, *2*, 4249.
(67) Petrovic, I.; Navrotsky, A.; Davis, M. E.; Zones, S. I. *Chem. Mater.* **1993**, *5*, 1805.
(68) Boerio-Goates, J.; Stevens, R.; Hom, B. K.; Woodfield, B. F.; Piccione, P. M.; Davis, M. E.; Navrotsky, A. *J. Chem. Thermodyn.* **2002**, *34*, 205.
(69) Li, Q. H.; Navrotsky, A.; Rey, F.; Corma, A. *Microporous Mesoporous Mater.* **2003**, *66*, 365.
(70) Schoenitz, M.; Navrotsky, A.; Ross, N. *Phys. Chem. Miner.* **2001**, *28*, 57.
(71) Hu, Y. T.; Navrotsky, A.; Chen, C. Y.; Davis, M. E. *Chem. Mater.* **1995**, *7*, 1816.
(72) Trofymluk, O.; Levchenko, A. A.; Tolbert, S. H.; Navrotsky, A. *Chem. Mater.* **2005**, *17*, 3772.
(73) Ford, M. H.; Auerbach, S. M.; Monson, P. A. *J. Chem. Phys.* **2007**, 126.
(74) Johnson, G. K.; Tasker, I. R.; Howell, D. A.; Smith, J. V. *J. Chem. Thermodyn.* **1987**, *19*, 617.
(75) Akporiaye, D. E.; Price, G. D. *Zeolites* **1989**, *9*, 321.
(76) Kramer, G. J.; Deman, A. J. M.; Vansanten, R. A. *J. Am. Chem. Soc.* **1991**, *113*, 6435.
(77) Civalleri, B.; Zicovich-Wilson, C. M.; Ugliengo, P.; Saunders, V. R.; Dovesi, R. *Chem. Phys. Lett.* **1998**, *292*, 394.
(78) Burchart, E. D.; Verheij, V. A.; Vanbekkum, H.; Vandegraaf, B. *Zeolites* **1992**, *12*, 183.
(79) de Boer, K.; Jansen, A. P. J.; Vansanten, R. A. *Phys. Rev. B* **1995**, *52*, 12579.
(80) Foster, M. D.; Friedrichs, O. D.; Bell, R. G.; Paz, F. A. A.; Klinowski, J. *Angew. Chem., Int. Ed.* **2003**, *42*, 3896.
(81) Foster, M. D.; Friedrichs, O. D.; Bell, R. G.; Paz, F. A. A.; Klinowski, J. *J. Am. Chem. Soc.* **2004**, *126*, 9769.
(82) Foster, M. D.; Simperler, A.; Bell, R. G.; Friedrichs, O. D.; Paz, F. A. A.; Klinowski, J. *Nature Mater.* **2004**, *3*, 234.

(83) Sastre, G.; Pulido, A.; Corma, A. *Microporous Mesoporous Mater.* **2005**, *82*, 159.
(84) Greaves, G. N.; Meneau, F.; Kargl, F.; Ward, D.; Holliman, P.; Albergamo, F. *J. Phys.: Condens. Matter* **2007**, 19.
(85) Zwijnenburg, M. A.; Bromley, S. T.; Flikkema, E.; Maschmeyer, T. *Chem. Phys. Lett.* **2004**, *385*, 389.
(86) Zwijnenburg, M. A.; Bromley, S. T.; Foster, M. D.; Bell, R. G.; Delgado-Friedrichs, O.; Jansen, J. C.; Maschmeyer, T. *Chem. Mater.* **2004**, *16*, 3809.
(87) Zwijnenburg, M. A.; Bromley, S. T.; van Alsenoy, C.; Maschmeyer, T. *J. Phys. Chem. A* **2002**, *106*, 12376.
(88) Zwijnenburg, M. A.; Cora, F.; Bell, R. G. *J. Phys. Chem. B* **2007**, *111*, 6156.
(89) Henson, N. J.; Cheetham, A. K.; Gale, J. D. *Chem. Mater.* **1994**, *6*, 1647.
(90) Newton, M. D.; Gibbs, G. V. *Phys. Chem. Miner.* **1980**, *6*, 221.
(91) Ford, M. H.; Auerbach, S. M.; Monson, P. A. *J. Chem. Phys.* **2004**, *121*, 8415.
(92) Sastre, G.; Corma, A. *J. Phys. Chem. B* **2006**, *110*, 17949.
(93) Moloy, E. C.; Davila, L. P.; Shackelford, J. F.; Navrotsky, A. *Microporous Mesoporous Mater.* **2002**, *54*, 1.
(94) Iler, R. K. *The chemistry of silica: Solubility, polymerization, colloid and surface properties, and biochemistry*; Wiley: New York, 1979.
(95) Li, Q. H.; Yang, S. Y.; Navrotsky, A. *Microporous Mesoporous Mater.* **2003**, *65*, 137.
(96) Navrotsky, A.; Tian, Z. R. *Chem.—Eur. J.* **2001**, *7*, 769.
(97) Roy, B. N.; Navrotsky, A. *J. Am. Ceram. Soc.* **1984**, *67*, 606.
(98) Clearfield, A. *Chem. Rev.* **1988**, *88*, 125.
(99) Babel, S.; Kurniawan, T. A. *J. Hazard. Mater.* **2003**, *97*, 219.
(100) Lee, Y.; Kao, C. C.; Kim, S. J.; Lee, H. H.; Lee, D. R.; Shin, T. J.; Choi, J. Y. *Chem. Mater.* **2007**, *19*, 6252.
(101) Cailliez, F.; Trzpit, M.; Soulard, M.; Demachy, I.; Boutin, A.; Patarin, J.; Fuchs, A. H. *Phys. Chem. Chem. Phys.* **2008**, *10*, 4817.
(102) Desbiens, N.; Demachy, I.; Fuchs, A. H.; Kirsch-Rodeschini, H.; Soulard, M.; Patarin, J. *Angew. Chem., Int. Ed.* **2005**, *44*, 5310.
(103) Shim, S. H.; Navrotsky, A.; Gaffney, T. R.; MacDougall, J. E. *Am. Mineral.* **1999**, *84*, 1870.
(104) Alberti, A.; Galli, E.; Vezzalini, G.; Passaglia, E.; Zanazzi, P. F. *Zeolites* **1982**, *2*, 303.
(105) Hunger, J.; Beta, I. A.; Bohlig, H.; Ling, C.; Jobic, H.; Hunger, B. *J. Phys. Chem. B* **2006**, *110*, 342.
(106) Ross, S.; Olivier, J. P. *On physical adsorption*; Interscience Publishers: New York, 1964.
(107) Yang, S. Y.; Navrotsky, A. *Microporous Mesoporous Mater.* **2000**, *37*, 175.
(108) Lella, A. D.; Desbiens, N.; Boutin, A.; Demachy, I.; Ungerer, P.; Bellat, J.-P.; Fuchs, A. H. *Phys. Chem. Chem. Phys.* **2006**, *8*, 5396.
(109) Jost, S.; Fritzsche, S.; Haberlandt, R. *Stud. Surf. Sci. Catal.* **2002**, *142*, 1947.
(110) Armbruster, T.; Gunter, M. E. *Am. Mineral.* **1991**, *76*, 1872.
(111) Carey, J. W.; Bish, D. L. *Am. Mineral.* **1996**, *81*, 952.
(112) Faux, D. A. *J. Phys. Chem. B* **1999**, *103*, 7803.
(113) Navrotsky, A. *Trans. Am. Geophys. Union* **1975**, *56*, 1082.
(114) Kiseleva, I.; Navrotsky, A.; Belitsky, I. A.; Fursenko, B. A. *Am. Mineral.* **1996**, *81*, 658.
(115) Kiseleva, I.; Navrotsky, A.; Belitsky, I. A.; Fursenko, B. A. *Am. Mineral.* **1996**, *81*, 668.
(116) Kiseleva, I.; Navrotsky, A.; Belitsky, I.; Fursenko, B. *Am. Mineral.* **2001**, *86*, 448.
(117) Kiseleva, I. A.; Navrotsky, A.; Belitsky, I. A.; Fursenko, B. A. *Geochem. Int.* **2001**, *39*, 170.
(118) Fridriksson, T.; Bish, D. L.; Bird, D. K. *Am. Mineral.* **2003**, *88*, 277.
(119) Fridriksson, T.; Carey, J. W.; Bish, D. L.; Neuhoff, P. S.; Bird, D. K. *Am. Mineral.* **2003**, *88*, 1060.
(120) White, C. L. I. M.; Ruiz-Salvador, A. R.; Lewis, D. W. *Angew. Chem., Int. Ed.* **2004**, *43*, 469.
(121) Baur, W. H. *Am. Mineral.* **1964**, *49*, 697.
(122) Yang, S. Y.; Navrotsky, A.; Wilkin, R. *Am. Mineral.* **2001**, *86*, 438.
(123) Fialips, C. I.; Carey, J. W.; Bish, D. L. *Geochim. Cosmochim. Acta* **2005**, *69*, 2293.
(124) Bish, D. L.; Carey, J. W. *Natural Zeolites: Occurrence, Properties, Applications* **2001**, *45*, 403.
(125) Carey, J. W.; Bish, D. L. *Clays Clay Miner.* **1997**, *45*, 826.
(126) Valueva, G. P.; Goryanov, S. V. *Russ. Geol. Geophys.* **1992**, *33*, 68.
(127) Sun, P. P.; Deore, S.; Navrotsky, A. *Microporous Mesoporous Mater.* **2006**, *91*, 15.
(128) Desbiens, N.; Boutin, A.; Demachy, I. *J. Phys. Chem. B* **2005**, *109*, 24071.
(129) Smirnov, K. S.; van de Graaf, B. *J. Chem. Soc., Faraday Trans.* **1996**, *92*, 2475.
(130) Sun, P. P.; Navrotsky, A. *Microporous Mesoporous Mater.* **2008**, *109*, 147.
(131) Sun, P. P.; Navrotsky, A. *Microporous Mesoporous Mater.* **2008**, *111*, 507.
(132) Xu, H. W.; Zhang, Y. P.; Navrotsky, A. *Microporous Mesoporous Mater.* **2001**, *47*, 285.
(133) Tian, Z. R.; Xia, G. G.; Luo, J.; Suib, S. L.; Navrotsky, A. *J. Phys. Chem. B* **2000**, *104*, 5035.
(134) Robie, R. A.; Hemingway, B. S. Thermodynamic properties of minerals and related substances at 298.15 K and 1 bar (10^5 pascals) pressure and at higher temperatures; U.S. G.P.O.: Washington, DC, 1995.
(135) Kresge, C. T.; Leonowicz, M. E.; Roth, W. J.; Vartuli, J. C.; Beck, J. S. *Nature* **1992**, *359*, 710.
(136) Beck, J. S.; Vartuli, J. C.; Roth, W. J.; Leonowicz, M. E.; Kresge, C. T.; Schmitt, K. D.; Chu, C. T. W.; Olson, D. H.; Sheppard, E. W.; Mccullen, S. B.; Higgins, J. B.; Schlenker, J. L. *J. Am. Chem. Soc.* **1992**, *114*, 10834.
(137) Petrovic, I.; Navrotsky, A.; Chen, C. Y.; Davis, M. E. *Stud. Surf. Sci. Catal.* **1994**, *84*, 677.
(138) Trofymluk, O.; Levchenko, A. A.; Navrotsky, A. *J. Chem. Phys.* **2005**, *123*, 194509.
(139) Kruk, M.; Jaroniec, M.; Sayari, A. *Langmuir* **1997**, *13*, 6267.
(140) Kruk, M.; Jaroniec, M.; Ryoo, R.; Joo, S. H. *Chem. Mater.* **2000**, *12*, 1414.
(141) Fritsch, S.; Post, J. E.; Navrotsky, A. *Geochim. Cosmochim. Acta* **1997**, *61*, 2613.
(142) Rollmann, L. D.; Schlenker, J. L.; Kennedy, C. L.; Kennedy, G. J.; Doren, D. J. *J. Phys. Chem. B* **2000**, *104*, 721.
(143) Rollmann, L. D.; Schlenker, J. L.; Lawton, S. L.; Kennedy, C. L.; Kennedy, G. J.; Doren, D. J. *J. Phys. Chem. B* **1999**, *103*, 7175.
(144) Paik, W. C.; Shin, C. H.; Lee, J. M.; Ahn, B. J.; Hong, S. B. *J. Phys. Chem. B* **2001**, *105*, 9994.
(145) Han, B.; Lee, S. H.; Shin, C. H.; Cox, P. A.; Hong, S. B. *Chem. Mater.* **2005**, *17*, 477.
(146) Lawton, S. L.; Rohrbaugh, W. J. *Science* **1990**, *247*, 1319.
(147) Schmitt, K. D.; Kennedy, G. J. *Zeolites* **1994**, *14*, 635.
(148) Sabater, M. J.; Sastre, G. *Chem. Mater.* **2001**, *13*, 4520.
(149) Bu, X. H.; Feng, P. Y.; Stucky, G. D. *Chem. Mater.* **2000**, *12*, 1505.
(150) Cox, P. A.; Casci, J. L.; Stevens, A. P. *Farady Discuss.* **1997**, *106*, 473.
(151) Piccione, P. M.; Yang, S. Y.; Navrotsky, A.; Davis, M. E. *J. Phys. Chem. B* **2002**, *106*, 3629.
(152) Sastre, G.; Leiva, S.; Sabater, M. J.; Gimenez, I.; Rey, F.; Valencia, S.; Corma, A. *J. Phys. Chem. B* **2003**, *107*, 5432.
(153) Lewis, D. W.; Freeman, C. M.; Catlow, C. R. A. *J. Phys. Chem.* **1995**, *99*, 11194.
(154) Moini, A.; Schmitt, K. D.; Valyocsik, E. W.; Polomski, R. F. *Zeolites* **1994**, *14*, 504.
(155) Zones, S. I.; Nakagawa, Y.; Yuen, L. T.; Harris, T. V. *J. Am. Chem. Soc.* **1996**, *118*, 7558.
(156) Lewis, D. W.; Willock, D. J.; Catlow, C. R. A.; Thomas, J. M.; Hutchings, G. J. *Nature* **1996**, *382*, 604.
(157) Ferey, G.; Loiseau, T.; Lacorre, P.; Taulelle, F. *J. Solid State Chem.* **1993**, *105*, 179.
(158) Loiseau, T.; Ferey, G. *J. Solid State Chem.* **1994**, *111*, 403.
(159) Gerardin, C.; Loiseau, T.; Ferey, G.; Taulelle, F.; Navrotsky, A. *Chem. Mater.* **2002**, *14*, 3181.
(160) Liu, Q. Y.; Navrotsky, A.; Jove-Colon, C. F.; Bonhomme, F. *Microporous Mesoporous Mater.* **2007**, *98*, 227.
(161) Corma, A.; Navarro, M. T.; Rey, F.; Valencia, S. *Chem. Commun.* **2001**, 1486.
(162) Blasco, T.; Corma, A.; Diaz-Cabanas, M. J.; Rey, F.; Vidal-Moya, J. A.; Zicovich-Wilson, C. M. *J. Phys. Chem. B* **2002**, *106*, 2634.
(163) Corma, A.; Diaz-Cabanas, M.; Martinez-Triguero, J.; Rey, F.; Rius, J. *Nature* **2002**, *418*, 514.
(164) Li, Q. H.; Navrotsky, A.; Rey, F.; Corma, A. *Microporous Mesoporous Mater.* **2003**, *59*, 177.
(165) Li, Q. H.; Navrotsky, A.; Rey, F.; Corma, A. *Microporous Mesoporous Mater.* **2004**, *74*, 87.
(166) Annen, M. J.; Davis, M. E.; Higgins, J. B.; Schlenker, J. L. *J. Chem. Soc., Chem. Commun.* **1991**, 1175.
(167) Le, S. N.; Navrotsky, A. *J. Solid State Chem.* **2007**, *180*, 2443.
(168) Le, S. N.; Eng, H. W.; Navrotsky, A. *J. Solid State Chem.* **2006**, *179*, 3731.
(169) Hammond, R.; Barbier, J. *Acta Crystallogr., Sect. B* **1996**, *52*, 440.
(170) Ng, H. Y.; Harrison, W. T. A. *Microporous Mesoporous Mater.* **1998**, *23*, 197.
(171) Harrison, W. T. A.; Gier, T. E.; Stucky, G. D.; Broach, R. W.; Bedard, R. A. *Chem. Mater.* **1996**, *8*, 145.
(172) Nenoff, T. M.; Harrison, W. T. A.; Gier, T. E.; Stucky, G. D. *J. Am. Chem. Soc.* **1991**, *113*, 378.
(173) Le, S. N.; Navrotsky, A. *J. Solid State Chem.* **2008**, *181*, 20.
(174) Le, S.-N.; Navrotsky, A.; Pralong, V. *Solid State Sci.* **2008**, *10*, 761.

(175) Trofymluk, O.; Levchenko, A. A.; Navrotsky, A. unpublished results, **2009**.
(176) Schoeman, B. J. *Microporous Mesoporous Mater.* **1998**, *22*, 9.
(177) Schoeman, B. J.; Regev, O. *Zeolites* **1996**, *17*, 447.
(178) Rimer, J. D.; Lobo, R. F.; Vlachos, D. G. *Langmuir* **2005**, *21*, 8960.
(179) Rimer, J. D.; Trofymluk, O.; Navrotsky, A.; Lobo, R. F.; Vlachos, D. G. *Chem. Mater.* **2007**, *19*, 4189.
(180) Mintova, S.; Olson, N. H.; Bein, T. *Angew. Chem., Int. Ed.* **1999**, *38*, 3201.
(181) Mintova, S.; Olson, N. H.; Senker, J.; Bein, T. *Angew. Chem., Int. Ed.* **2002**, *41*, 2558.
(182) Mintova, S.; Olson, N. H.; Valtchev, V.; Bein, T. *Science* **1999**, *283*, 958.
(183) Hould, N. D.; Lobo, R. F. *Chem. Mater.* **2008**, *20*, 5807.
(184) Davis, T. M.; Drews, T. O.; Ramanan, H.; He, C.; Dong, J. S.; Schnablegger, H.; Katsoulakis, M. A.; Kokkoli, E.; McCormick, A. V.; Penn, R. L.; Tsapatsis, M. *Nature Mater.* **2006**, *5*, 400.
(185) de Moor, P. P. E. A.; Beelen, T. P. M.; Komanschek, B. U.; Beck, L. W.; Wagner, P.; Davis, M. E.; van Santen, R. A. *Chem.—Eur. J.* **1999**, *5*, 2083.
(186) Dokter, W. H.; Vangarderen, H. F.; Beelen, T. P. M.; Vansanten, R. A.; Bras, W. *Angew. Chem., Int. Ed.* **1995**, *34*, 73.
(187) Kirschhock, C. E. A.; Buschmann, V.; Kremer, S.; Ravishankar, R.; Houssin, C. J. Y.; Mojet, B. L.; van Santen, R. A.; Grobet, P. J.; Jacobs, P. A.; Martens, J. A. *Angew. Chem., Int. Ed.* **2001**, *40*, 2637.
(188) Watson, J. N.; Iton, L. E.; Keir, R. I.; Thomas, J. C.; Dowling, T. L.; White, J. W. *J. Phys. Chem. B* **1997**, *101*, 10094.
(189) Kumar, S.; Davis, T. M.; Ramanan, H.; Penn, R. L.; Tsapatsis, M. *J. Phys. Chem. B* **2007**, *111*, 3398.
(190) Cundy, C. S.; Forrest, J. O.; Plaisted, R. J. *Microporous Mesoporous Mater.* **2003**, *66*, 143.
(191) Liang, D.; Follens, L. R. A.; Aerts, A.; Martens, J. A.; Van Tendeloo, G.; Kirschhock, C. E. A. *J. Phys. Chem. C* **2007**, *111*, 14283.
(192) Drews, T. O.; Tsapatsis, M. *Microporous Mesoporous Mater.* **2007**, *101*, 97.
(193) Yang, S. Y.; Navrotsky, A. *Chem. Mater.* **2002**, *14*, 2803.
(194) Yang, S. Y.; Navrotsky, A.; Wesolowski, D. J.; Pople, J. A. *Chem. Mater.* **2004**, *16*, 210.
(195) Atkins, P. W. *Physical chemistry*, 6th ed.; Freeman: New York, 1998.
(196) Landry, C. C.; Tolbert, S. H.; Gallis, K. W.; Monnier, A.; Stucky, G. D.; Norby, F.; Hanson, J. C. *Chem. Mater.* **2001**, *13*, 1600.
(197) Tolbert, S. H.; Landry, C. C.; Stucky, G. D.; Chmelka, B. F.; Norby, P.; Hanson, J. C.; Monnier, A. *Chem. Mater.* **2001**, *13*, 2247.
(198) Zones, S. I.; Vannordstrand, R. A. *Zeolites* **1988**, *8*, 409.
(199) Zones, S. I.; Vannordstrand, R. A. *Zeolites* **1988**, *8*, 166.
(200) Subotic, B.; Skrtic, D.; Smit, I.; Sekovanic, L. *J. Cryst. Growth* **1980**, *50*, 498.
(201) Gross, A. F.; Yang, S.; Navrotsky, A.; Tolbert, S. H. *J. Phys. Chem. B* **2003**, *107*, 2709.
(202) Liu, Q. Y.; Navrotsky, A. *Geochim. Cosmochim. Acta* **2007**, *71*, 2072.
(203) Rimer, J. D.; Vlachos, D. G.; Lobo, R. F. *J. Phys. Chem. B* **2005**, *109*, 12762.
(204) Rino, J. P.; Ebbsjo, I.; Kalia, R. K.; Nakano, A.; Vashishta, P. *Phys. Rev. B* **1993**, *47*, 3053.
(205) Du, M. H.; Kolchin, A.; Cheng, H. P. *J. Chem. Phys.* **2004**, *120*, 1044.
(206) Devine, R. A. B.; Dupree, R.; Farnan, I.; Capponi, J. J. *Phys. Rev. B* **1987**, *35*, 2560.
(207) Brinker, C. J.; Kirkpatrick, R. J.; Tallant, D. R.; Bunker, B. C.; Montez, B. *J. Non-Cryst. Solids* **1988**, *99*, 418.
(208) Chuang, I. S.; Maciel, G. E. *J. Phys. Chem. B* **1997**, *101*, 3052.
(209) Civalleri, B.; Casassa, S.; Garrone, E.; Pisani, C.; Ugliengo, P. *J. Phys. Chem. B* **1999**, *103*, 2165.

CR800495T